





Hydrology of Wetlands

July

TR 2009/095

Auckland Regional Council
Technical Report No.095 July 2009
ISSN 1179-0504 (Print)
ISSN 1179-0512 (Online)
ISBN 978-1-877540-08-0

Technical Report, first edition.

| Reviewed by: | Approved for ARC publication by: |
|-----------------------------------------------------------------------------------|------------------------------------------------------------------------------------|
|  |  |
| Name: Claudia Hellberg | Name: Paul Metcalf |
| Position: Stormwater Advisor Stormwater Action Team | Position: Group Manager Environmental Programmes |
| Organisation: Auckland Regional Council | Organisation: Auckland Regional Council |
| Date: 12 August 2010 | Date: 23 September 2010 |

Recommended Citation:

SEMADENI-DAVIES, A., 2009. Hydrology of Wetlands. Prepared by NIWA Ltd for Auckland Regional Council. Auckland Regional Council Technical Report 2009/095.

© 2009 Auckland Regional Council

This publication is provided strictly subject to Auckland Regional Council's (ARC) copyright and other intellectual property rights (if any) in the publication. Users of the publication may only access, reproduce and use the publication, in a secure digital medium or hard copy, for responsible genuine non-commercial purposes relating to personal, public service or educational purposes, provided that the publication is only ever accurately reproduced and proper attribution of its source, publication date and authorship is attached to any use or reproduction. This publication must not be used in any way for any commercial purpose without the prior written consent of ARC. ARC does not give any warranty whatsoever, including without limitation, as to the availability, accuracy, completeness, currency or reliability of the information or data (including third party data) made available via the publication and expressly disclaim (to the maximum extent permitted in law) all liability for any damage or loss resulting from your use of, or reliance on the publication or the information and data provided via the publication. The publication and information and data contained within it are provided on an "as is" basis.

Hydrology of Wetlands

Annette Semadeni-Davies, PhD

Prepared for
Auckland Regional Council

© All rights reserved. This publication may not be reproduced or copied in any form without the permission of the client. Such permission is to be given only in accordance with the terms of the client's contract with NIWA. This copyright extends to all forms of copying and any storage of material in any kind of information retrieval system.

NIWA Client Report: **AKL-2007-017**
October 2009

NIWA Projects: ARC07135

National Institute of Water & Atmospheric Research Ltd
269 Khyber Pass Road
Newmarket, Auckland
PO Box 109695, Auckland
Phone: +64 9 375 2050, Fax: +64 9 375 2051
www.niwa.co.nz

Contents

| | | |
|----------|----------------------------------------------------|-----------|
| 1 | Executive Summary | 1 |
| 2 | Introduction | 3 |
| 2.1 | Background | 3 |
| 2.2 | Objectives | 6 |
| 3 | Site Descriptions | 7 |
| 3.1 | Longford Park, Papakura | 7 |
| 3.2 | Wainoni Wetland 2, Pitoitoi Ave, Greenhithe | 11 |
| 4 | Model Description | 14 |
| 4.1 | Input data (Input.xls) | 16 |
| 4.2 | Radiation sub-model (Radiation.xls) | 17 |
| 4.2.1 | Solar (shortwave) radiation | 18 |
| 4.2.1.1 | Solar geometry | 18 |
| 4.2.1.2 | Incoming solar radiation | 21 |
| 4.2.1.3 | Exposed, full sun | 22 |
| 4.2.1.4 | Shade and sky-view near vertical structures | 23 |
| 4.2.2 | Longwave radiation | 25 |
| 4.2.2.1 | Atmospheric longwave radiation | 25 |
| 4.2.2.2 | Surface longwave radiation | 25 |
| 4.2.2.3 | Net allwave radiation | 26 |
| 4.3 | Turbulent heat flux sub-model (Turbulent flux.xls) | 26 |
| 4.3.1 | Water temperature | 27 |
| 4.3.2 | Latent heat, evaporation and evapotranspiration | 30 |
| 4.3.2.1 | Open water | 30 |
| 4.3.2.2 | Vegetation | 31 |
| 4.3.3 | Sensible heat | 32 |
| 4.4 | Flow sub-model (Flow.xls) | 33 |
| 5 | Results with Discussion | 38 |
| 5.1 | Radiation | 38 |

| | | |
|----------|----------------------------------------------------|-----------|
| 5.1.1 | Longford Park | 38 |
| 5.1.2 | Wainoni Wetland 2 | 41 |
| 5.2 | Water temperature | 42 |
| 5.2.1 | Longford Park | 42 |
| 5.2.2 | Wainoni Wetland 2 | 43 |
| 5.3 | Turbulent fluxes and evapotranspiration | 46 |
| 5.3.1 | Longford Park | 46 |
| 5.3.2 | Wainoni Wetland 2 | 49 |
| 5.4 | Flow reduction and attenuation | 51 |
| 5.4.1 | Longford Park | 51 |
| 5.4.2 | Wainoni Wetland 2 | 53 |
| 5.5 | Implications for water management | 55 |
| 5.5.1 | Water temperature | 55 |
| 5.5.2 | Evaporation and evapotranspiration | 56 |
| 5.5.3 | Flow | 56 |
| 6 | Conclusions | 58 |
| 7 | Recommendations for Calibration and Testing | 60 |
| 7.1 | Radiation | 60 |
| 7.2 | Water temperature | 61 |
| 7.3 | Evapotranspiration | 61 |
| 7.4 | Flow | 62 |
| 8 | References | 64 |

1 Executive Summary

This project was commissioned by the Auckland Regional Council (ARC) and accompanies a coupled energy and water balance spread-sheet model that has been applied to two wetlands. Wainoni Wetland 2 and Longford Park were chosen by the ARC as they represent the types of wetland covered in TP 10 (trapezoid and banded bathymetry). Aside from bathymetry, the wetlands have different catchment areas and land use, dimensions, outflow structures, layouts and emergent vegetation, all of these factors affect both their energy and water balances. The main objective was to determine whether wetlands are more effective at controlling stormwater peak flows and reducing flow volumes than ponds. Evaporation from open water and evapotranspiration from emergent wetland vegetation were thus prime considerations.

This report describes the model including its organisation into sub-models, parameters and calculations. The model was used to simulate outflow from the wetlands with and without emergent vegetation. The latter was undertaken to allow a comparison with detention ponds of the same dimensions under the assumption that the two types of detention facility differ hydrologically only in evapotranspiration. As the model has not been calibrated, the findings listed below are tentative.

- The model is sensitive to the parameters which govern solar radiation absorption by open water relative to emergent vegetation (ie, shading and sky-view).
- Outflow for each wetland is governed by the storage available and the size and type of the outlet structure.
- The emergent vegetation has a greater latent heat flux than open water, particularly at Longford Park where the reeds could extend 1.2 m above the water surface. The difference is not as noticeable at Wainoni Wetland 2 where emergent vegetation is only a few centimetres high. However, this finding is tentative because the evapotranspiration sub-model is very sensitive to stomatal resistance.
- There is little difference in the simulated evaporative losses for ponds and wetlands despite the difference in latent heat between open water and emergent vegetation. The lack of difference is due to several factors including the relative areas of open water to emergent vegetation, and changing patterns of shading for each type of detention facility.
- Simulated water temperature at Longford Park tracks the average daily air with a one or two day lag. The water temperature is on average 2°C warmer than the daily average air temperature because of heating by solar radiation.
- Simulated water temperature at Wainoni Wetland 2 is sensitive to the height of the bank vegetation which shades both the water surface and the emergent vegetation. There is a seasonal difference in water temperature (cooler in winter and warmer in summer) compared to air temperature.

- Water temperature is sensitive to the water depth: Wainoni Wetland 2 (depth 0.5 m) has a greater diurnal range of temperatures and responds more rapidly to changes in air temperature than Longford Park (1.5 m depth of open water pools).
- Evaporative losses do not have a significant effect on simulated high flows. The Longford Park simulations found that peak flows during wet periods were largely unaffected by evaporation. During dry periods (ie, summer) the pond simulations had several events which were, however, not present in the wetland simulations. Wainoni Wetland 2 was not simulated for high summer, even so, the flow event in late December 2006 was present in the pond simulations but not the wetland simulations.
- Longford Park, which is the larger of the two wetlands, is better able to attenuate peak flows. Wainoni Wetland 2 has a large outlet structure despite its small size which means that the simulated outflow was almost instantaneous and inflows peaks were released in the next timestep.

The report makes the following recommendations for monitoring to refine model calibration.

As a minimum, we recommend monitoring:

- inflow and outflow rate,
- water temperature,
- for one calendar year,
- at Longford Park which has inflow and outflow structures more suitable for monitoring.

Flows would be used to assess evaporative losses directly. The combination of flow and temperature at the inlet and outlet can be used as a proxy for the energy balance.

An alternative, but more costly, exercise would involve monitoring energy fluxes directly. This is feasible using apparatus operated by NIWA, Hamilton. It would significantly increase the reliability of the model especially its ability to simulate the effects of shade and sheltering.

2 Introduction

2.1 Background

The ARC is committed to the principles of low impact urban design and development (LIUDD) for stormwater management. LIUDD requires local control of stormwater quantity and quality to safeguard local receiving environments from the negative impacts of urbanisation. Design principles and criteria stormwater control are given in TP 124 (ARC, 2000) and TP 10 (ARC, 1992, 2003) which recommend a suit of systems for source, site and catchment control. These have a range of sizes and functions and should be carefully chosen for local needs. Two popular, end-of-pipe (site or catchment control) facilities for attenuating peak flows and treating stormwater quality are wet ponds and constructed wetlands. Both systems work by detaining stormwater flows following rain events. Each consists of a permanent pool of water into which stormwater is directed and temporarily stored. Outflow from the pool is controlled by an outlet structure such as an orifice or weir. Once the volume of stormwater overtops the invert level of the outlet, water is slowly released.

While detained, natural physical, chemical and biological processes treat the stormwater. Sediment settling is the major removal process of both wetlands and ponds. However, wetlands have the potential to increased removal efficiencies, especially for fine sediment fractions (Bavor *et al.*, 2001; Wong *et al.*, 1999) due to the presence of vegetation. This is important in Auckland as many of the metal contaminants in the city's stormwater are associated with fine particulate matter (Timperley *et al.*, 2001). Vegetation can improve sediment (and contaminant) removal by slowing velocities, decreasing turbulence (and therefore promoting plug-flow), and trapping sediments, rubbish and debris. The large surface area of plants also provides a surface for microbial growth which can increase adsorption rates of dissolved and fine particulate contaminants. The many processes in operation has lead to wetlands often being equated to the "kidneys" of the environment (Mitsch and Gosselink, 1993) due to their ability to cycle nutrients, alleviate floods and provide water for low-flow and groundwater recharge.

Over and above their value for water treatment and flow attenuation, the ARC favours constructed wetlands over ponds for a variety of reasons including:

- Compensation for drained natural wetlands.
- Landscaping and recreation.
- Habitat creation and encouragement of biodiversity.

This project has been commissioned by the ARC to determine whether wetlands designed according to TP 10 are more effective at controlling flow than ponds. Detention in ponds and wetlands slows the hydrograph response and attenuates flow into natural receiving waters. Of concern to the ARC is the fact that stormwater can

contribute to downstream channel and bed erosion – this means that design criteria for flow control should include adequate storage to avoid erosion in receiving streams. Elliott *et al.* (2004) investigated the erodibility of bed and bank materials for streams across Auckland. They found that erodibility varied considerably both from stream to stream and at different sites for the same stream, the variability encountered could not be explained. There was some indication that erodibility increased with clay content. It was found that erosion begins at a critical near-bed (50 mm from the bed) velocity of approximately 0.15 m/s and increases linearly with velocity (1.0 cm/min per cummec of flow). A general form for the erosion-shear stress relationship was proposed by Jowett and Elliot (2006) to use in the absence of more specific information, erosion requires a shear stress of 33 N/m² and increases linearly (0.005 – 0.01 kg/m²/s).

The ARC has called for the development and running of a physically-based hydrological model which can simulate the outflow of stormwater wetlands constructed and sized according to the design criteria set out in TP 10 (ARC, 2003). The ARC requested that evapotranspiration from the wetland be incorporated into the model as the potential losses could have an impact on wetland outflows by lowering the water level of the wetland during dry periods thus increasing the pre-event water storage available. Part of the rationale for this study is the notion that wetland plants can have a negative stomatal resistance to evapotranspiration. This, in conjunction with the greater exposure wetland plants to the atmosphere than the water surface suggests that wetlands can potentially have greater water losses than open water in ponds. If it can be shown that wetlands do potentially offer better protection for downstream receiving waters, then the ARC would have a further reason to favour wetland construction over wet detention ponds.

Evapotranspiration is the composite of water losses to the atmosphere and is equated to the latent heat flux to the atmosphere divided by the latent heat of vaporization. Evapotranspiration from a wetland will have a number of sources and pathways: evaporation from bare soil at the wetland margins, evaporation from free water (either free water on vegetation or open water on the water pools), and transpiration from vegetation (ie, through stomata). Here, evaporation from open water is calculated using the Penman equation and evaporation from the wetland vegetation using the Penman-Monteith Equation.

Of additional interest is the effect of wetlands on the temperature of stormwater flowing through the wetland. Indeed, the ARC, in conjunction with the University of Auckland, is running a related research project to measure water temperature in a number of stormwater wetlands. The temperature of water bodies is affected by inflows and outflows, exchange of heat at the air-water interface (short- and long-wavelength irradiative inputs, long-wavelength irradiative emissions, evaporation, conduction, and convection), depth penetration by solar radiation, heat conduction to and from the underlying sediments, and mixing by wind. For a given net surface heat flux the temperature change is inversely proportional to water depth and consequently for a deep water body the thermal response is low. As wetlands are shallow, the response is likely to be greater with rapid warming and cooling.

Water temperature is calculated here in order to determine evaporation from the open water surface of the wetland. The warmer the water, the greater the evaporative

losses from open water. Warming of stormwater can have two other impacts on wetland function: as viscosity (and density) is a function of temperature, sediment fall velocities can be increased leading to faster settling rates; on the other hand, warm water is able to hold less dissolved oxygen (DO) – this can affect biological activity in the wetland and can lead to oxygen depletion in downstream habitats. The 1992 ANZECC Guidelines recommended that DO should not normally be permitted to fall below 6 mg/l determined over at least one diurnal cycle. At 6 mg/l DO is around 50 per cent saturation at 8°C, but around 66 per cent for 20°C.

While open stormwater systems have been used to cool urban areas through the release of latent heat, the USEPA (1999) warns that shallow wetlands can act as a heat sink which results in further warming of stormwater. This has proved the case for agricultural wetlands (J. C. Rutherford, NIWA, Hamilton, unpublished data for Echidna Creek, Southeastern Queensland). Rutherford *et al.* (1997: 2004) too found that water in small streams can heat up rapidly during the day as water moves downstream although they also cool rapidly at night. Maxted *et al.* (2005) found similar rapid heating and cooling in shallow Auckland streams. They discussed the implications of heating of streams downstream of constructed ponds, including for stormwater management, and found that pond discharge can have negative impacts on local biota. Rutherford *et al.* (1997: 2004) and Maxted *et al.* (2005) noted that the impact of banks and riparian vegetation on water temperature diminishes with the width of the water body in relation to the height of the vegetation.

Solar radiation is a major heat source during daylight hours. Solar radiation can be split into two parts, direct and diffuse. The former refers to parallel beams of solar radiation from the sun to Earth. The latter refers to solar radiation that has scattered from the direct beam as a result of molecules and aerosols (notably water vapour in clouds) in the atmosphere. Clear, sunny days have the greatest potential for heating (and evaporation), however, heating is sensitive to shading by banks and riparian vegetation. A water body in the southern hemisphere lying to the south of a east-west aligned strip of vegetation will be cooler than one lying to the north. During cloudy days, incoming solar radiation is restricted to diffuse beam and the effects of shading are not as noticeable. Cooling of open water is mostly due to the release of longwave radiation, particularly during cold clear nights when the water can be warmer than the surrounding air.

Aside from shading, vegetation and banks also reduce the sky-view of the water body which can lower both the long- and diffuse shortwave radiation available irrespective of pond orientation to the sun. Imagine lying on the ground perpendicular to a wall of infinite extent vertically and horizontally with the top of your head touching the wall, theoretically, only half of the sky dome will be visible. This means, assuming an isotropic radiance distribution (ie, equal radiative emissions from all parts of the sky dome), the diffuse solar and atmospheric longwave radiation reaching you will also be halved.

2.2 Objectives

This project aims to:

- Develop a coupled wetland flow and energy balance model that simulates continuous water temperature, evapotranspiration rates and flow through wetlands.
- Run the model for two wetlands designed according to TP 10 identified by the ARC with different catchment and design characteristics: ie, Longford Park, Papakura (banded bathymetry) and Wainoni Wetland 2, Greenhithe (trapezoid bathymetry).
- Compare event and long-term inflow and outflow volumes and flow rates to give an indication of flow attenuation and discharge reduction to quantify the impact of wetlands on downstream hydrology. The model will be run with vegetation and without to ascertain the importance of wetland plants to evapotranspiration, storage and outflow.
- Recommend a monitoring programme for model calibration depending on the model results and with consultation in the ARC.

3 Site Descriptions

Both wetlands were chosen in consultation with the ARC and are also being monitored as part of an MSc research programme into the differences in water temperature for ponds and wetlands (Chung and Fassman, 2006) University of Auckland. The wetlands are fairly typical of constructed stormwater wetlands in Auckland that have been designed according to TP 10. They are both rather small and are situated in new greenfield developments as part of the landscaping. Longford Park is an example of a banded bathymetry wetland while Wainoni Wetland 2 is an example of trapezoid bathymetry.

With the exception of rainfall, climate data for the wetland energy balance and flow model comes from the NIWA National Climate Database.

3.1 Longford Park, Papakura

The Longford Park wetland (Figures 1, 2 and 3) was originally a wet detention pond constructed in a reserve by developers at the time of subdivision in the late 1990s. It was subsequently converted into a banded wetland by the Papakura District Council (resource consent prepared by Harrison Grierson, 2003). Design details are given in the resource consent. The original pond was designed for a water quality 24-hour storage of 3580 m³ according to the criteria laid out in TP 108 (ARC, 1999) and TP 10 (ARC, 1992). While the construction of submerged ridges for planting reduced the depth of the detention basin and therefore storage, it was none-the-less felt by the council that the addition of wetland vegetation would improve the overall removal efficiency of the facility as well as the aesthetics of the reserve where it is situated.

The wetland takes water from a new subdivision consisting of low-density housing (single storey bungalows). Figure 1 is an aerial photograph of the original pond with respect to the catchment area taken in 2001. The figure was down loaded from the ARC map site (http://maps.arc.govt.nz/website/maps/map_general.htm - accessed 18 October 2009). The wetland is offline and drains into the Pahurehure Inlet of the Manukau Harbour near the Southern Motorway. The area is now fully developed. The catchment has an area of 27.5 ha, the length is 0.62 km with an average slope of 0.01 m/m. The impervious surface contributing to flow is 17 ha – of which 80 per cent consists of residential surfaces (eg, roofs) and 19 per cent roads. The run-off coefficient for these surfaces is 0.96 and the time of concentration is estimated to be 15 minutes. The run-off coefficient for the 10.5 ha of permeable surfaces is 0.59 and the time of concentration is half an hour.

The wetland is roughly rectangular (90x30 m, surface area 2673 m², volume at overflow 2328 m³) and consists of three permanent pools (depth 1.5 m) separated by two vegetated submerged ridges (depth 0.3 m). The ratio of open water pool to submerged ridge is approximately 47 to 53 per cent respectively when the water level is at the invert level of the outlet. The pools and ridges are fairly evenly spaced along

the length of the basin. The banks surrounding the wetland have a slope of around 1:4 and are thickly planted with tall rushes and the wetland is surrounded by native rushes, NZ flax and grasses on the banks. The height of both the rushes and marginal plants is around 1.2 m.

Flow comes directly from stormwater pipes and there is little to no baseflow. The inflow structure is a culvert that leads to a short riprap channel. The outflow is via a rectangular concrete lined spillway of 3 m width. Flow through the spillway is controlled by a 1.5 m wide weir with its base at the level of the channel. The invert level is 1.5 m.

The coupled energy and water balance model was set with a one-hour timestep for Longford Park. The model was run from January 2004 to December 2006. Flow to the wetland was simulated by the ARC for this project using the BECA flow model (continuous curve number method). Rain data for the flow model comes from Row St, Onehunga, the gauge is administered by the ARC. Climate data comes from Auckland Airport and consists of hourly ambient air temperature, wind speed and cloud coverage.

Figure 1

Aerial photograph of the original wet detention pond (ringed) showing wetland location and catchment land use, note that the surrounding area is now fully developed (photo from the ARC map website, 2001 image).



Figure 2

Rushes planted on submerged ridges (0.3 m depth) have split the original pond into three pools of open water of around 1.5 m depth. Water is able to flow freely through the reeds. The pond margins are planted with riparian vegetation. (photos by J. Moores, NIWA, 2006).

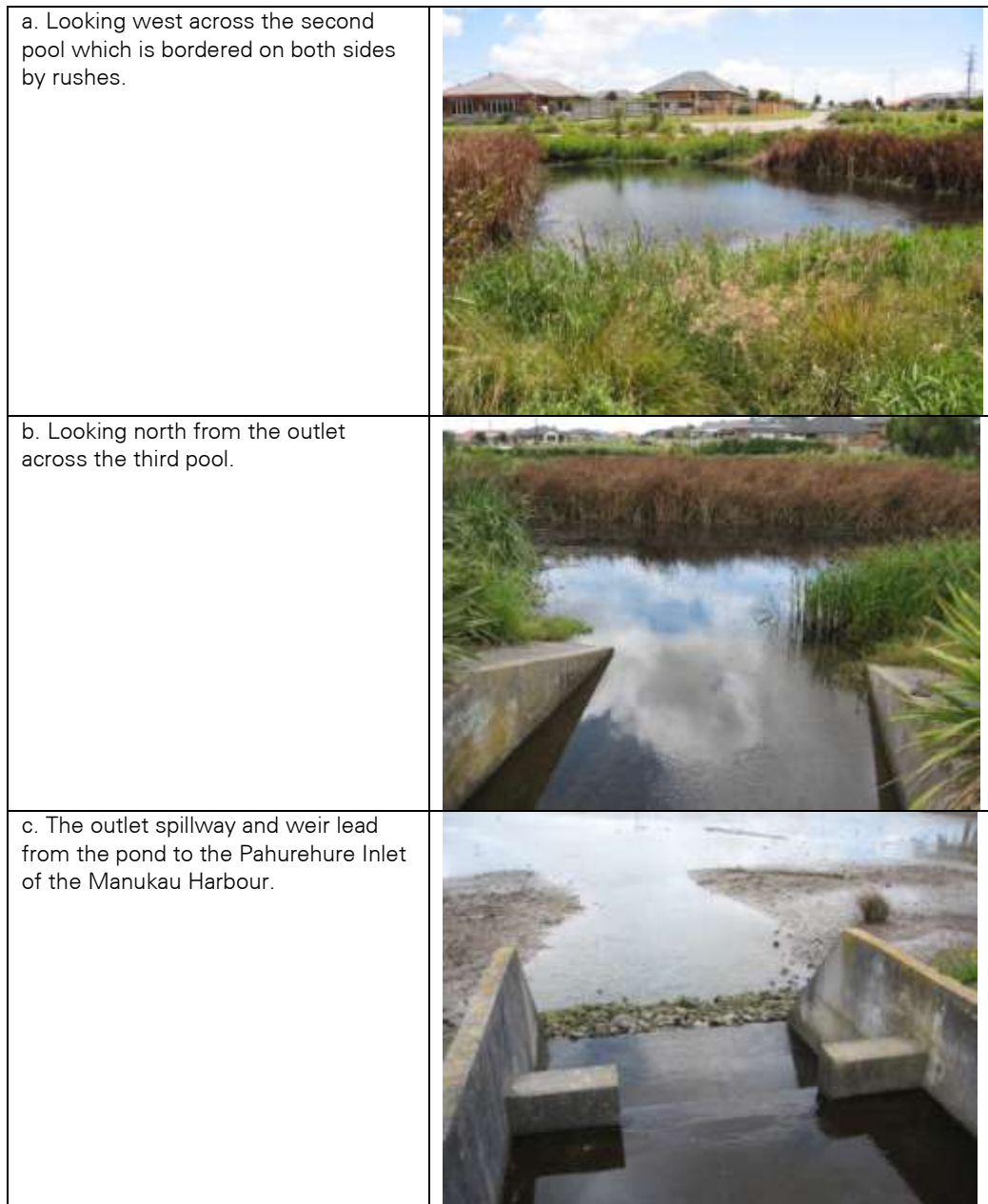
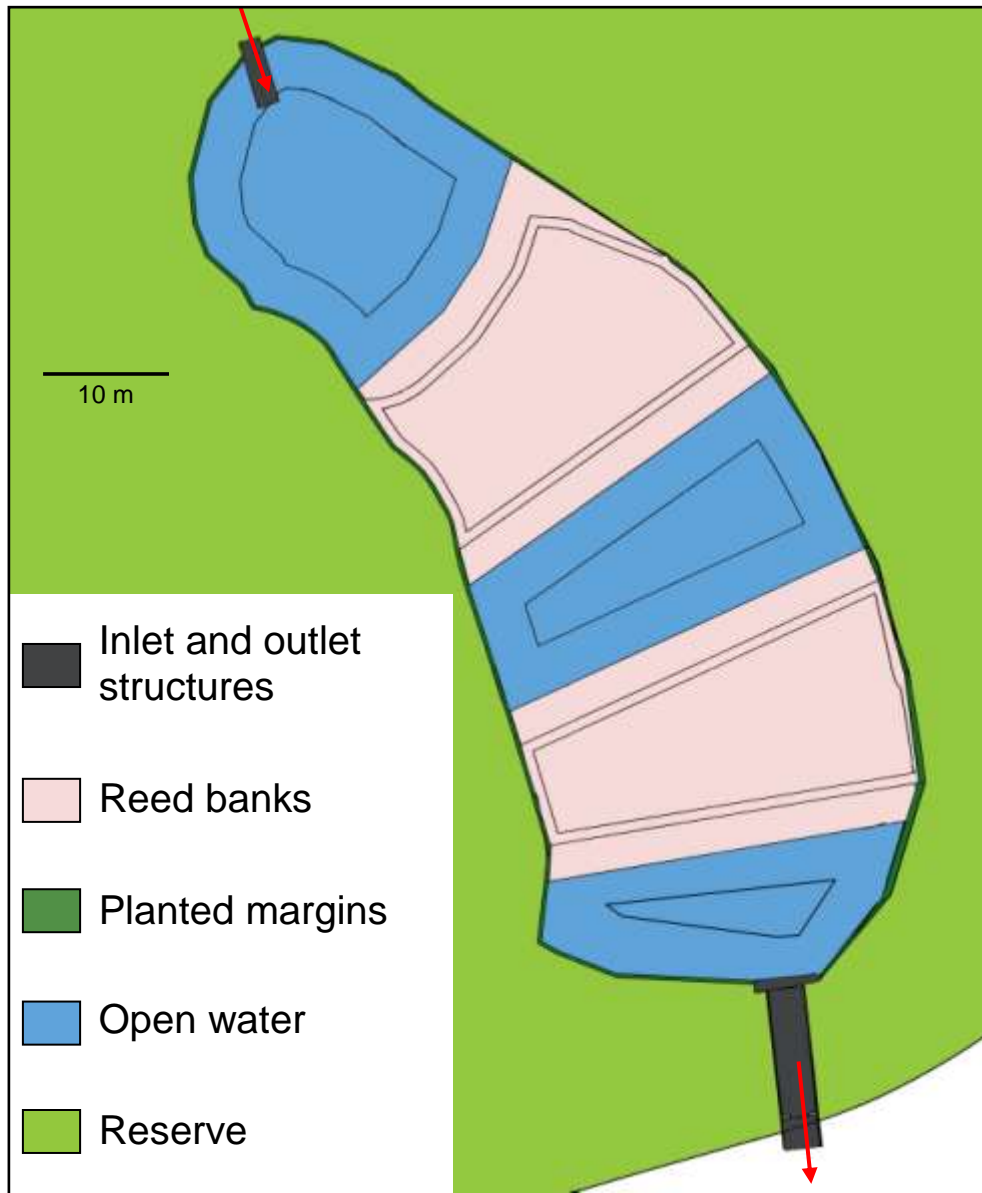


Figure 3

Sketch of Longford Park wetland showing the layout of the vegetated ridges and the open water pools (after resource consent).



3.2 Wainoni Wetland 2, Pitoitoe Ave, Greenhithe

Wainoni Wetland 2, is one of three wetlands servicing a development that was constructed in 2000 by Universal Homes in accordance to TP 10 (ARC, 1992). Two of the wetlands are side by side (Figure 4). These are called the Eastern and Western Marshes in the development documentation (original plans, 1998 and later maintenance schedules 2001 – both prepared by Harrison Grierson), but are known by ARC as Wainoni Wetlands 1 and 2 respectively. Figure 4 was down loaded from the ARC (http://maps.arc.govt.nz/website/maps/map_general.htm - accessed 18 October 2009). Wetlands 1 and 2 are on a narrow terrace some 6 m above sea level within a steep sided valley. Both these wetlands are offline and their outflow drains via a Waiora filter into the Te Wharau Creek which is a tidal tributary of the Upper Waitemata Harbour. When Figure 4 was taken in 2001, the area was undergoing development and the wetlands had not been planted. The area is now fully developed: the building density is greater than for Longford Park and the houses are mostly two storeys.

Figure 4

Aerial photograph of Wainoni Wetland 2 (inset ringed) during construction showing wetland location and catchment land use, note that the surrounding area is now fully developed (photo from the ARC map website, 2001 image).



The wetland dimensions used as parameters in the model come from the wetland maintenance schedule (Harrison Grierson, 2001). According to the schedule the total catchment area for the two wetlands is 4 ha, stormwater flowing to Wetland 2 comes from an area of 3.2 ha, half of which is covered in impervious surfaces. Flows includes water from catchpits and stormwater pipes as well as any overland flow. The time of concentration is estimated to be 10 minutes.

Wainoni Wetland 2 is small having a wet storage volume of only 140 m³ and a live storage of 500 m³ (Figures 5 and 6). The wetland has a total basin area of 335 m², however, at overflow the approximate dimensions are 7x42 m (294 m²). The wetland has a bank slope of 1:3. The average depth is around 0.5 m (determined from the cross-sectional area provided in the first draft of the maintenance schedule, supplied by the ARC). The wetland has been planted with emergent vegetation such as jointed twig rush, spike rush and club rush. Despite the best efforts of pukeko (swamp hens) documented in the maintenance schedule, the wetland is almost completely vegetated. The ratio of open water to vegetation is around 20 per cent to 80 per cent (see Figure 6). The height of the emergent vegetation above the permanent water level ranges from just a few centimetres to half a metre. Marginal plants are well established native shrubs including cabbage tree, toetoe, koromiko and NZ flax.

Inflow is via a 750 mm pipe at the eastern corner of the wetland. Here there is a headwall outlet structure of about 1 m depth filled with riprap. The basin also receives baseflow and overland flow from the surrounding area. Outflow is via a 1800 mm diameter circular standpipe, this is connected to a 675 mm diameter outlet pipe. The standpipe has a debris screen consisting of 30 bars (2 cm diameter) arranged tepee fashion around the rim, and is surrounded by low vegetation which has choked the outlet in places (Figure 6).

Figure 5

Sketch of Wainoni Wetland 2 showing inlet and outlet structures (modified from maintenance schedule, Harrison Grierson, 2001).

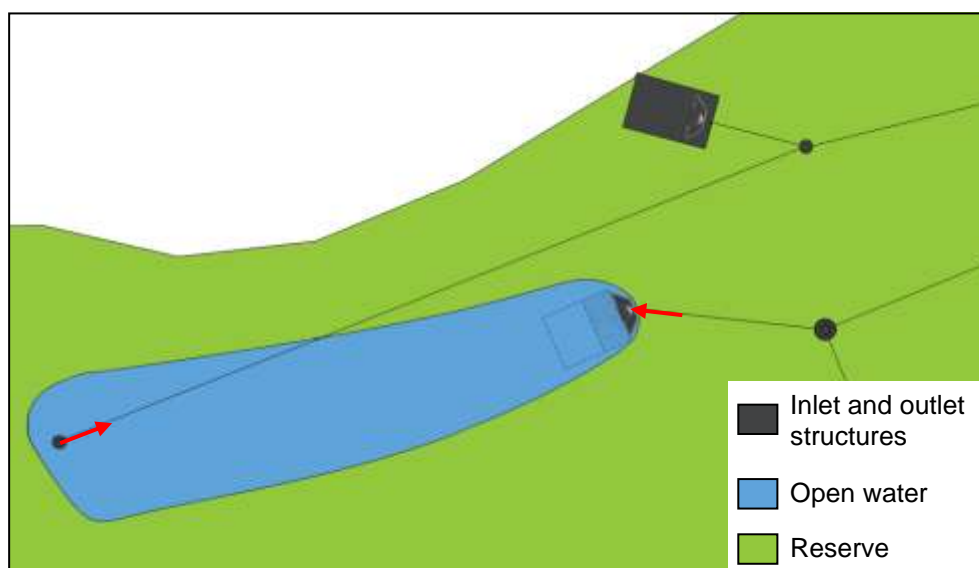


Figure 6

Wainoni Wetland 2, the Western Marsh, showing emergent and marginal vegetation (photos by J. Moores, NIWA, 2006).



Wainoni Wetland 2 is small and the hydrological response is fairly rapid in comparison to Longford Park, hence the model timestep is 10 minutes. The period modelled is July to December 2006. Flow to the wetland was simulated by the ARC for this project using the BECA flow model. Rain data for the flow model comes from Oteha at Rosedale Ponds, the gauge is administered by the ARC. Climate data comes from the high resolution observations made in Kumeu. Air temperature and wind speed are available at 10 minute intervals. Cloud data is only available hourly, time intervals between hours were assigned the hourly value.

4 Model Description

The model consists of four coupled spreadsheets (MS Excel 7), one for data management (Input.xls) and three sub-models for simulating the wetland energy balance (Radiation.xls and Turbulent Fluxes.xls) and water balance (Flow.xls).

The spreadsheets are protected and only those cells highlighted green can be altered. The sub-model worksheets are arranged in the same format and are labelled:

- parameters – this worksheet contains the constants used in the sub-model;
- input data – data are read directly from the Input.xls spreadsheet;
- calculation worksheets – the simulation routines described below are found in separate worksheets; and
- summary charts – model outputs for each sub-model are graphed as time series.

The variables and parameters in each of the spreadsheets have been given descriptions including units and names.

The model solves the governing equations for the water and energy balances given below. The two balances are linked through evaporation from open water and evapotranspiration from the vegetation. The energy balance in relation to wetland hydrology is shown in Figure 7 and the way in which the spreadsheets are coupled is shown in Figure 8.

Figure 7

Energy and flow terms simulated in the model with respect to wetland hydrology.

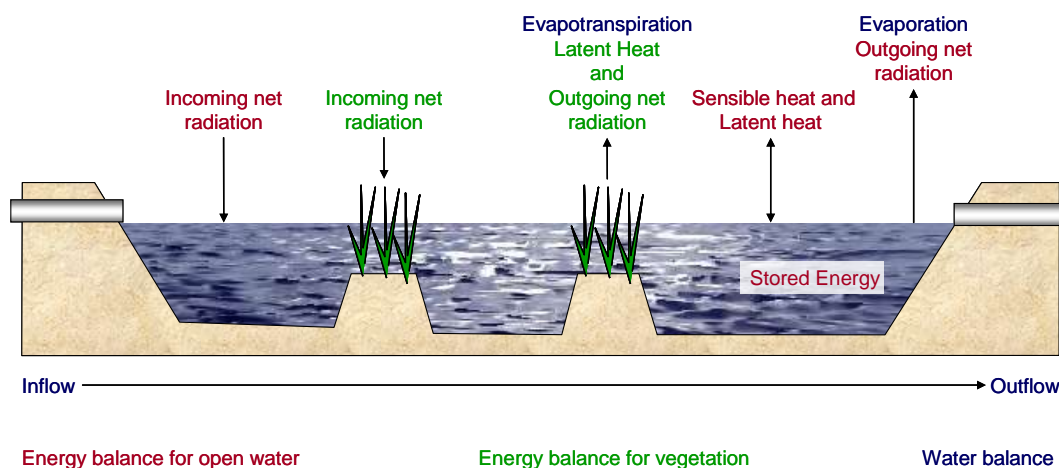
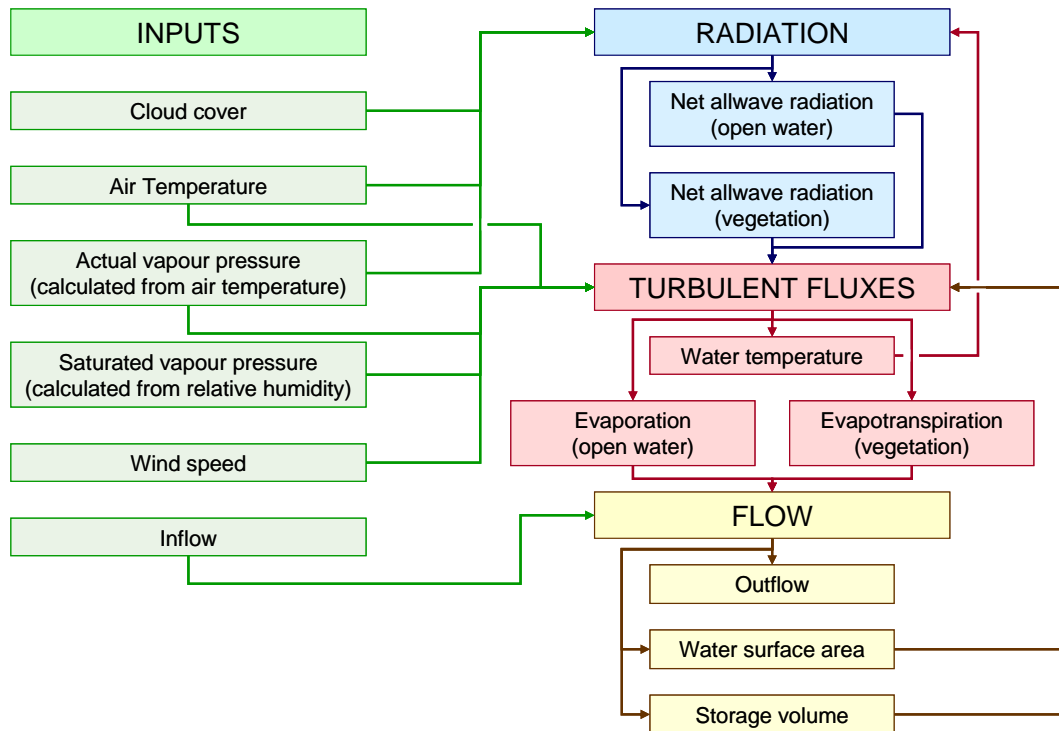


Figure 8

Schematic overview of coupling between the input and sub-model spreadsheets.



Water balance

Flow through the wetland is calculated as a function of the wetland water balance. Water flow paths within the wetland are not simulated. Conceptually, wetland outflow can be determined by the relationship between inflow, the change in storage volume and the hydraulic head above the outlet structure. The size of the outflow structure aperture determines the outflow rate and the height of the invert level determines the maximum dead storage available. The wetland water balance can be written as:

$$F_{out} = F_{in} - ET_v - ET_w \pm \Delta S \quad \text{Equation 1}$$

Where F_{in} and F_{out} are inflow and outflow rate, ET_v is evapotranspiration rate from the wetland vegetation, ET_w is evaporation rate from the open water surface and ΔS is the rate of change in the volume of water stored in the wetland. All terms have the unit m^3/h .

Energy balance

There are two energy balance sub-models (Figure 8): Radiation and Turbulent Heat Fluxes. Within each, the routines are split into separate sets of calculations for the vegetated surfaces and open water. The energy sub-models are lumped for each surface so that water is treated as a single pool and vegetation as a single canopy. This method has drawbacks, calculating shadows is an obvious case in point. Moreover, the approach assumes that there is full horizontal and vertical mixing in the open water. The energy balance of water under the emergent vegetation is not

modelled. However, using a fully-distributed model would lead to undue complexity and spurious accuracy.

The energy balance for open water can be written as (eg, Henderson-Sellers, 1984, Finch and Gash, 2002):

$$\Delta Q_S = Q^*_W + Q_G + Q_P \pm Q_{EW} \pm Q_{HW} \pm Q_A \quad \text{Equation 2}$$

Where ΔQ_S is the change in energy stored in the water body, Q^*_W is net allwave radiation flux absorbed by the water, Q_G is conductive heat flux from the base of the wetland to the water, Q_P heat flux from rain falling directly on the water, Q_{EW} is latent heat flux of vaporisation for open water, Q_{HW} is sensible heat flux for open water and Q_A is heat flux advected into and out of the wetland via inflow and outflow. All units are W/m^2 . Q_G , Q_A and Q_P are considered negligible and are not calculated here.

For the vegetation, only Q^*_V (net allwave radiation flux absorbed by the vegetation canopy) and Q_{EV} (evapotranspiration flux) are calculated in the model.

4.1 Input data (Input.xls)

This spreadsheet is the only one that allows the user to add or change data and is used for data management. The sub-models read input data directly from this spreadsheet, although the data are repeated in the sub-model spreadsheets for the user as an aid to understanding. Input data are summarised in Table 1.

Table 1

Input data used in the wetland coupled energy balance, flow model.

| Data set | Symbol | Unit | Source |
|-------------------------------|--------|---------|---------------------------------------------------------------------------------------|
| Cloud cover | cloud | tenths* | NIWA climate data |
| Air temperature | T_a | °C | NIWA climate data |
| Relative humidity | RH | % | NIWA climate data |
| Wind speed | u | m/s | NIWA climate data |
| Inflow | F_i | m/h | ARC flow simulations |
| Saturated air vapour pressure | e_o | Pa | Calculated as: $e_o = 610.8e^{\left(\frac{17.27T_a}{T_a+237.3}\right)}$ Equation 3 |
| Actual air vapour pressure | e_a | Pa | Calculated as: $e_a = \frac{RH e_o}{100}$ Equation 4 |

* Standard cloud cover observations are in eights and must be converted to tenths.

4.2 Radiation sub-model (Radiation.xls)

All objects with a temperature above absolute zero Kelvin (-273.15 °C), that is, possessing energy, emit radiation as a result of the motion of their molecules. The amount of energy emitted is proportional to the fourth power of the objects surface temperature (Kelvin) and is related to a range of wavelengths. Increases in temperature are met by increases in energy but decreases in wavelengths so that objects with high temperatures have shorter wavelengths but greater radiative emissions. The portion of the electromagnetic spectrum which is of most interest for atmospheric applications lies between 0.1 and 100 μm , this section is split into two broad bands; longwave and shortwave. Shortwave radiation originates from the Sun (ca. 6000 K) and covers the range 0.15 to 4 μm with a peak at 0.5 μm , while longwave radiation is associated with cooler earthly temperatures (233 - 313 K) and lies in the range 3 to 100 μm (infrared) with a peak at 11.4 μm . Hence, shortwave radiation is variously known as solar radiation and longwave radiation as infrared or terrestrial radiation. In the Radiation sub-model, there are separate worksheets for both sets of calculations. Model inputs and parameters are given in Tables 2 and 3 below, the model outputs are the net allwave radiation for water and vegetation respectively (W/m^2).

The sub-model does not take the local topography into account in order to simplify calculations. This assumption is acceptable for the Langford Park site which is located on relatively flat land with very few surrounding trees and houses some distance away. However, Wainoni Wetland 2 is located on a small terrace in the valley of a steep sided tidal estuary. This means that there a possibility of shading during the morning and evening and diminished sky-view at the wetland. The first is self explanatory, the second refers to the proportion of the sky-dome which is visible to the wetland. Sky-view is important when determining both the diffuse solar radiation and incoming longwave radiation.

Table 2

Inputs for the radiation sub-model.

| Input | Symbol | Unit | Source |
|----------------------------|--------|--------|----------------------|
| Air temperature | T_a | °C | Input.xls |
| Cloud cover | cloud | tenths | Input.xls |
| Actual air vapour pressure | e_a | Pa | Input.xls |
| Water temperature | T_w | °C | Turbulent fluxes.xls |

Table 3

Parameters for the radiation sub-model.

| Parameter | Symbol | Value | Unit | Input status |
|---------------------------------------------|--------------|-----------------------|----------------------------------|------------------------------------------------------|
| Solar constant | I_0 | 1367 | W/m ² | Unchangeable |
| Latitude | ϕ | Variable | degrees | User defined (automatically converted to radians) |
| Longitude | Long | Variable | degrees | User defined (automatically converted to radians) |
| Emissivity of water | ϵ_w | 0.95 | - | Unchangeable |
| Refractive index for water | Ri | 1.333 | - | Unchangeable |
| Albedo of water for diffuse solar radiation | α_w | 0.2 | - | Unchangeable |
| Emissivity of vegetation | ϵ_v | 0.90 | - | Unchangeable |
| Albedo of vegetation | α_v | 0.16 | - | Unchangeable |
| Stefan-Boltzman constant | σ | 5.67x10 ⁻⁸ | W/m ² /K ⁴ | Unchangeable |
| Transmissivity of the atmosphere | ψ | 0.84 | | Unchangeable |
| Cloud coefficients (shortwave) | a | 0.02 | | Unchangeable |
| | b | 0.95 | | |
| | c | 1.2 | | |
| Cloud coefficient (longwave) | d | 0.17 | - | Unchangeable |
| Sky-view | SKY | Variable | | Calculated (equation 17) |
| Height of vegetation | H_v | Variable | m | User defined |
| Width of open water bands | B_w | Variable | m | User defined |

4.2.1 Solar (shortwave) radiation

While measurements of global solar radiation are available from the NIWA national climate data base, diffuse and direct beam incoming solar radiation are calculated in the model in order to simulate the effects of shading and reduced sky-view due to vegetation on water temperature and evaporation. The effects of multiple reflections and absorption by the sides of the vegetation layer are not simulated.

4.2.1.1 Solar geometry

In order to calculate incoming solar radiation it is necessary to know the relative position of the Sun to the particular point of interest on the local horizontal surface. The geometrical relationship is complicated by the facts that:

- the Earth's orbit around the Sun is elliptical, the *perihelion* (when Earth is closest to the Sun) is during the Northern Hemisphere winter and the *aphelion* (furthest from the Sun) during summer;

- the Earth is tilted by 23.5 °, the *axial tilt* is responsible for varying day-lengths so that during the perihelion the Arctic is in darkness and the Antarctic enjoys constant sunshine, the opposite is true for the aphelion.

The actual solar irradiance at the top of the atmosphere can be determined using trigonometric functions for spheres based on the following angles with respect to a given location, x , on the Earth's surface (Figure 9):

The *latitude*, ϕ , of a location is the angle between the equatorial plane and a line taken from the site to the centre of the plane. The angle is assigned a positive value in the Northern Hemisphere and a negative value in the Southern Hemisphere. Latitude is important for the calculation of both the length of the day and the distance travelled by the oblique rays of the Sun.

The *longitude*, λ , is the angle from meridian for point x to the Greenwich or Prime Meridian (where $\lambda=0$). **Longitude ranges from +180° eastwards and -180° westwards.**

The *solar declination*, δ , is the angle between the solar beam, taken from the centre of the Sun, and the centre of the equatorial plane, that is, the latitude at which the Sun is directly overhead. The declination can be found using the following approximation (note that the calculations below are in radians):

$$\delta = \text{radians} \left(-23.4 \cos \left[\frac{360 J + 10}{365} \right] \right) \quad \text{Equation 5}$$

Where J is the *Julian day*, the number of the day of the year (January 1 = 1, January 2 = 2 etc.). Michalsky (1988) states that this approximation is accurate to around 2°, which is adequate for most applications. The Julian day is read from the date using a specific Excel function for this purpose.

The *zenith direction* lies directly above the location and is the extension of the line from the centre of the equatorial plane through the point. It is at right angles to the local horizontal surface. The *zenith angle*, Z , is the angle between the zenith direction and the Sun-to-site line.

$$\cos(Z) = \sin(\delta) + \sin(\phi) + \cos(\delta) \cos(\phi) \sin(h) \quad \text{Equation 6}$$

The *solar elevation*, β , is the angle between the Sun-to-site line and the local surface horizontal. It is the complementary angle to the zenith angle.

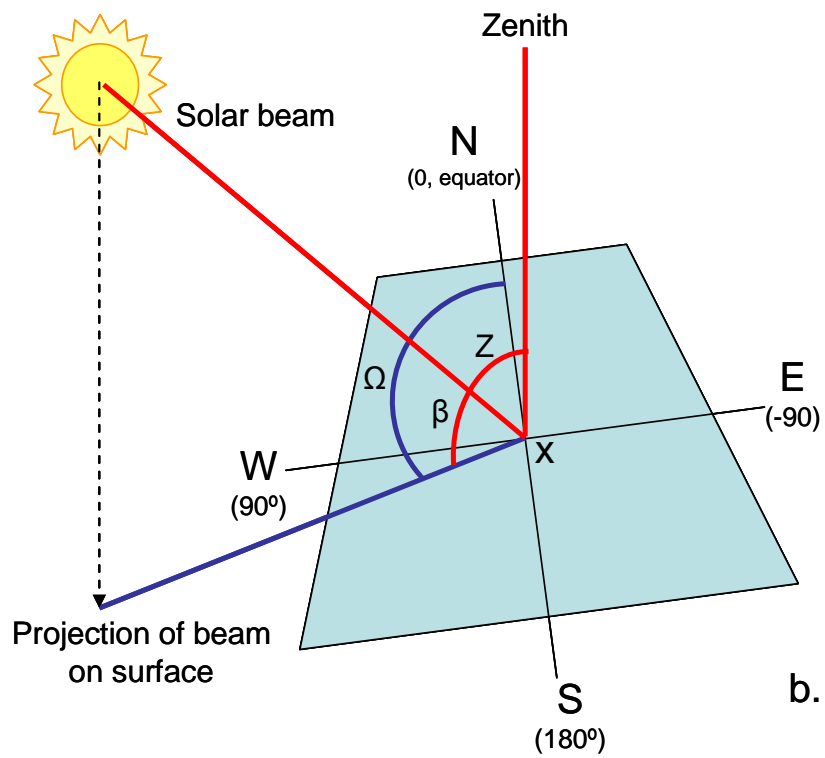
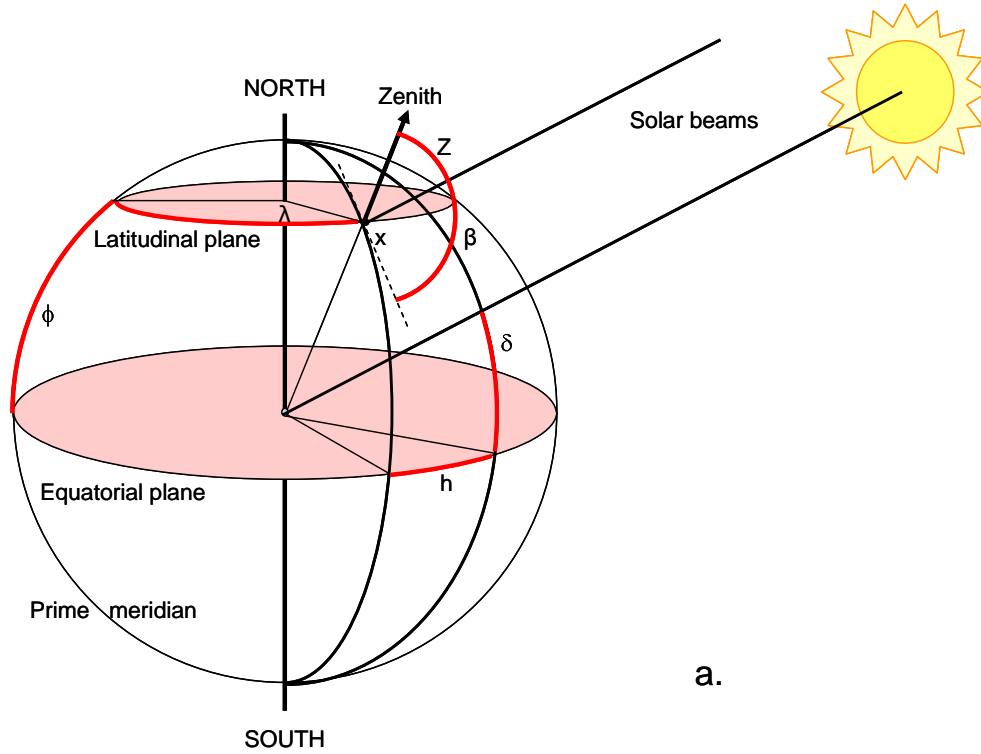
The *hour angle*, h , is the angle that the Earth must turn so that the meridian of point of location is directly under the Sun. This angle is a function of the time of day and can be written as:

$$h = \frac{\pi (12 - LAST)}{12} \quad \text{Equation 7}$$

Where $LAST$ is the *local apparent solar time* in 24-hour clock. The local standard time corrected for longitude (*local mean solar time, LMST*), differs from the local solar time by a small amount called the *equation of time, ET*, due to the Earth's differing rate of rotation caused by its eccentric orbit. The equation of time can be approximated by:

Figure 9

Solar geometry for a point x on a horizontal surface for the globe: a. in relation to the globe; and b. in relation to the surface, azimuth for southern hemisphere.



$$ET = 9.87 \sin(2B) - 7.53 \cos(B) - 1.5 \sin(B) \quad \text{Equation 8}$$

Where

$$B = \frac{2\pi (L - 81)}{364}$$

Given that each hour is equivalent to 15° of Earth rotation, the local standard time, *LST* (ie, daylight savings removed) can be corrected to LMST in the following way:

$$LMST = LST \pm 4 \text{ minutes } (\lambda - \text{standard time zone meridian} \times 15) \quad \text{Equation 9}$$

That is, four minutes are added for every degree longitude east of the standard meridian (or subtracted for every degree west). In New Zealand, the local standard time zone meridian is +12 hours from Greenwich mean time (ie, the Prime Meridian). The local apparent solar time is then:

$$LAST = LMST + ET \quad \text{Equation 10}$$

For completeness, although not calculated in the model, the *solar azimuth*, Ω , is the direction of the solar beam (Figure 9b). It is usually defined as the angle between due south and the projection onto the local horizontal plane of the Sun-to-site line, so that an angle facing south (ie, the equator for the northern hemisphere) is zero, 180° north and 90° and 270° west and east. The azimuth angle can also be defined in terms of the equator, thus in the Southern Hemisphere, the azimuth is calculated from due north so that the angle facing the equator remains zero. Under this convention, west is positive and east negative.

It should also be noted that the zenith and azimuth angles change for sloped surfaces depending on the slope angle and orientation of the surface to the sun. As this model is for water and the vegetation canopy, it is assumed that all surfaces are horizontal

4.2.1.2 Incoming solar radiation

The extraterrestrial solar radiation, K_{EX} , received at any time and location at the top of the atmosphere is calculated as a function of the zenith angle (equation 6) and the solar constant ($I_o = 1367 \text{ W/m}^2$) which is the radiation that would be received if the sun were directly overhead:

$$K_{EX} = I_o \cos(Z) \quad \text{Equation 11}$$

The shielding effect of the atmosphere means that globally an average of only 54 per cent of the shortwave radiation incident at the top of the atmosphere reaches the ground surface (Henderson-Sellers and Robinson, 1986). More specifically, once the extraterrestrial solar radiation for a certain time and location is known, the global radiation at the surface can be estimated according to the atmospheric conditions. The usual approach is to estimate $K_{\downarrow 0}$, the incoming shortwave radiation under clear skies, according to known or assumed relationships for absorption, scattering and reflection by the atmospheric constituents. With detailed models and appropriate data it is possible to calculate $K_{\downarrow 0}$ to an accuracy within 5 per cent, unfortunately, data

constraints ensure that less rigorous statistical methods are often applied (Oke, 1987). $K\downarrow_0$ can be approximated as:

$$K\downarrow_o = K_{EX} \left(\psi^{\left(\frac{1}{\cos(Z)} \right)} \right) \quad \text{Equation 12}$$

Where ψ is the atmospheric transmissivity which dependent on the concentration of gases, water vapour and aerosols in the air. For cloudless, pollution free air, ψ is around 0.9, and for smoggy or hazy skies it is around 0.6. A typical value, and that adopted here, is 0.84 (Campbell, 1977).

Direct beam solar radiation, $K\downarrow_s$, is calculated using an empirical relationship of for a horizontal surface:

$$K\downarrow_s = K\downarrow_o \left(a + b \left(\frac{n}{N} \right)^c \right) \quad \text{Equation 13}$$

Where a , b and c are empirical constants with the values 0.02, 0.95 and 1.2 respectively and n/N is the ratio of recorded sunshine hours, n , to the maximum astronomically possible, N . This ratio is related to the average daily cloud fraction, *cloud* (the proportion of cloud cover expressed in tenths from zero for clear skies to unity for overcast skies), as $n/N = 1 - \text{cloud}$. The direct beam radiation is then used to calculate the other solar radiation terms separately for the two surfaces (water and vegetation) of the wetland.

4.2.1.3 Exposed, full sun

It was assumed that the emergent vegetation at Longford Park is not subjected to shading or the effects of reduced sky-view. Direct beam solar radiation reaching the vegetation canopy is taken directly from equation 13 (ie, $K\downarrow_{SV} = K\downarrow_s$). Diffuse solar radiation is calculated empirically as:

$$K\downarrow_{DV} = 0.38 K\downarrow_o - K\downarrow_{SV} \cos(Z) \quad \text{Equation 14}$$

Global incoming solar radiation at the vegetation canopy ($K\downarrow_v$) is the sum of the direct and diffuse beam solar radiation.

Not all the solar radiation reaching the canopy is available for evapotranspiration. Some of this radiation is reflected back into space. The ratio of solar radiation reaching a surface to that reflected back into space is known as the surface's albedo, α . Albedo is related to colour with lighter substances reflecting more shortwave radiation than darker objects. Net solar radiation for the vegetation canopy (that is, solar radiation available for evapotranspiration) is thus calculated as:

$$K^*_v = K\downarrow_v (1 - \alpha_v) \quad \text{Equation 15}$$

Where α_v is the albedo of the vegetation, set here to 0.2, a low value for vegetation which is used to approximate the dark rushes and shrubs found at the wetlands.

4.2.1.4 Shade and sky-view near vertical structures

Vertical structures (in the case of the wetlands: vegetation) reduce the solar radiation reaching a horizontal surface in two ways: a. shading, b. shielding the horizontal surface from exposure to the sky-dome. The former is self-explanatory latter is the so-called sky-view discussed above.

At Longford Park, the emergent vegetation is assumed not to be shaded, while the water surface is subject to shading by marginal and emergent vegetation, both of which are roughly the same height (1.2 m) above the water surface. At Wainoni Wetland 2, which is narrow, both the emergent vegetation and the water surface are shaded by the marginal vegetation. The marginal vegetation, including the banks of the wetland, stands at about 2 m above the wetland surface. The emergent vegetation is predominantly low, only a few centimetres, and will have minimal effect on the open water.

Diffuse solar radiation reaching the horizontal surface (ie, open water at Longford Park and both emergent vegetation and open water at Wainoni Wetland 2) is calculated from the direct beam solar radiation (equation 13) as:

$$K \downarrow_{DW} = 0.38 \downarrow_o - K \downarrow_s \cos(Z) SKY \quad \text{Equation 16}$$

Where SKY is sky-view.

The geometry of vegetation to the wetland resembles a canyon and the average (median) sky-view factor is approximated as:

$$SKY = 0.5 \left(1 + 0.5 \cos \left[\tan^{-1} \left(\frac{H_v}{B_w / 4} \right) \right] - 0.5 \right) + 0.5 \left(1 + 0.5 \cos \left[\tan^{-1} \left(\frac{H_v}{3B_w / 4} \right) \right] - 0.5 \right) \quad \text{Equation 17}$$

Where H_v is the height of the vegetation and B_w is the width of the area subject to the vertical structure. This calculation gives the median sky-view for the surface as an approximate average, obviously, some points on the surface will have full exposure.

At Longford Park, the landscape is flat and vegetation in and around the wetland is low (1.2 m) compared to the open water, hence sky-view increases rapidly towards the centre of the band so that the impact of vegetation on sky-view is negligible. An open water band width of 16 m was chosen for the calculation which is the average width of the three pools found at Longford Park, this gives a sky-view factor of around 0.98 for the open water surface.

The situation at Wainoni Wetland 2 is more complex due to the wetland's location in a valley. Only the effect of the marginal vegetation, which is around 1.5 m above the wetland surface, is taken into account here. The emergent vegetation in the wetland itself is fairly low and will have a minimal impact on sky-view at the water surface. Using equation 16 and assuming an average wetland width of 7 m surrounded by the marginal vegetation, the sky-view for both the emergent vegetation and open water is around 0.86.

The effect of shading on direct beam solar radiation reaching the wetland ($K_{\downarrow_{sw}}$) is treated simplistically as a function of the solar zenith angle and the height of the vertical structure. In reality, the degree of shading is also a function of the solar azimuth angle with respect to the location and orientation of the structure. Again, for Longford park, the calculation of shading is made for only the water surface while for Wainoni Wetland 2, the calculation is made for both the water surface and the emergent vegetation. The direct beam solar radiation (equation 13) is reduced by the ratio of the shadow length to the width of the open water band.

$$K_{\downarrow_{sw}} = K_{\downarrow_s} \left(1 - \frac{SL}{B_w} \right) \quad \text{Equation 18}$$

Where SL is the length of a shadow cast by the vegetation on the water surface. SL is calculated from vegetation height (H_v) and the zenith angle as:

$$SL = \frac{H_v}{\tan\left(\frac{\pi}{2} - Z\right)} \quad \text{Equation 19}$$

Thus, for Longford Park, if the shadow cast by the rushes is 8 m long, then the direct beam solar radiation for open water is reduced by about 50 per cent. Obviously, in reality this situation would lead to half the water being in full sun and half with no direct beam solar radiation. It is assumed that the net effect on water temperature and evaporation would be the same.

Reflected solar radiation for the emergent vegetation at Wainoni Wetland 2 is calculated as above for Longford Park using equation 15 with an albedo of 0.2. The solar radiation absorbed by the water is calculated separately for the direct and diffuse solar inputs. This is because the albedo of water is related to the incidence angle of the beam. For diffuse beam solar radiation, a constant albedo, α_{Dw} , of 0.2 is used under the assumption that diffuse radiation is isotropic. The situation for direct beam solar radiation is quite different and decreases with the angle of incidence. Assuming calm water with no waves which can change the local zenith, the angle of incidence of the direct beam is equivalent to the solar zenith angle. At midday when the sun is overhead (zenith angle ≈ 0), the reflected direct beam solar radiation will be minimal. In contrast, in the early morning and late afternoon when the sun is low above the horizon, much of the direct beam radiation will be reflected by the water. Water albedo for direct beam solar radiation is calculated using Fresnel's law:

$$\alpha_{sw} = \frac{1}{2} \left[\frac{\sin^2 \theta - R}{\sin^2 \theta + R} + \frac{\tan^2 \theta - R}{\tan^2 \theta + R} \right] \quad \text{Equation 20}$$

Where R is the angle of refraction which is calculated from Snell's law as:

$$R = \sin^{-1} \left(\frac{\sin \theta}{R_i} \right) \quad \text{Equation 21}$$

Where R_i is the refractive index of water which is 1.333 at 20°C.

The net solar radiation for water is then:

$$K^*_w = K \downarrow_{DW} (1 - \alpha_{DW}) + K \downarrow_{SW} (1 - \alpha_{SW}) \quad \text{Equation 22}$$

4.2.2 Longwave radiation

At temperatures typical of the Earth's surface, the radiation emitted is in the infrared waveband and can be determined using the Stefan-Boltzmann Law adjusted for emissivity. The equation is the same for both the Earth's surface and atmosphere, however, the emissivity differs with solid objects having a higher value than the atmosphere. The relative difference in emissivity means that, under the assumption that the air and surface temperature are similar, incoming longwave radiation from the atmosphere is less than outgoing longwave radiation from the surface so that the net longwave radiation, L^* is negative in most cases.

4.2.2.1 Atmospheric longwave radiation

Atmospheric or incoming longwave calculations should take into account the different temperatures and emissivities of clouds and aerosols at different levels. However, this approach is impractical and the atmosphere is assumed to have a typical bulk value emissivity and air temperature. The clear sky incoming longwave radiation is given as:

$$L \downarrow_o = \sigma \epsilon_o (e_a + 273.15)^4 \quad \text{Equation 23}$$

Where σ is the Stefan-Boltzmann constant ($5.67 \times 10^{-8} \text{ W m}^{-2} \text{ K}^{-4}$) and ϵ_o is atmospheric emissivity calculated from air temperature and actual vapour pressure (e_o) according to Idso (1981) as:

$$\epsilon_o = 0.7 + 5.95 \times 10^{-5} \frac{e_a}{100} e^{\left(\frac{1500}{T_a + 273.15} \right)} \quad \text{Equation 24}$$

Clouds are almost full infrared radiators, so it stands to reason that their presence has a drastic effect on longwave radiation. The clear sky incoming longwave radiation is modified for cloud using an empirical relationship (Oke, 1987). At Longford Park there are separate calculations for vegetation and water:

$$L \downarrow_v = L \downarrow_o (1 - d \text{ cloud})^2 \quad \text{Equation 25}$$

$$L \downarrow_w = L \downarrow_o (1 - d \text{ cloud})^2 \text{ SKY} \quad \text{Equation 26}$$

Where d is a coefficient for cloud type, a typical value of 0.17 is used here. At Wainoni Wetland 2, the emergent vegetation is also affected by the bank vegetation and the calculation for both the water surface and the emergent vegetation are the same (Equation 26).

4.2.2.2 Surface longwave radiation

The calculations for outgoing longwave radiation emitted by vegetation and water are identical except for the temperature input and the choice of emissivity:

$$L \uparrow_v = \sigma \varepsilon_v T_v^4 + 273.15^4 \quad \text{Equation 27}$$

$$L \uparrow_w = \sigma \varepsilon_w T_w^4 + 273.15^4 \quad \text{Equation 28}$$

Where $L \uparrow_v$ and $L \uparrow_w$ are outgoing longwave radiation from vegetation and water respectively, T_v is vegetation temperature (assumed to be equivalent to air temperature), T_w is water temperature (calculated in the Turbulent Fluxes sub-model), ε_v is the vegetation emissivity (0.90) and ε_w is the water emissivity (0.95).

The net longwave radiation, L^* , for vegetation and water are:

$$L^*_v = L \downarrow_v - L \uparrow_v \quad \text{Equation 29}$$

$$L^*_w = L \downarrow_w - L \uparrow_w \quad \text{Equation 30}$$

4.2.2.3 Net allwave radiation

Net allwave radiation absorbed by each surface is the sum of the net solar radiation and net longwave radiation for that surface:

$$Q^*_v = K^*_v + L^*_v \quad \text{Equation 31}$$

$$Q^*_w = K^*_w - L^*_w \quad \text{Equation 32}$$

4.3 Turbulent heat flux sub-model (Turbulent flux.xls)

The turbulent heat fluxes of latent and sensible heat are driven by the vertical gradients of wind velocity, ambient air temperature and humidity. Wind is a major driver of both fluxes. The sub-model assumes a logarithmic wind profile with stable conditions. The effects of barriers to wind flow (eg, vegetation, banks) is not simulated. The sensible heat flux has an effect on temperature and is able to be sensed with a thermometer whereas the latent or stored heat flux is the energy needed to change the phase of water. The convention is that positive fluxes are from the surface while negative fluxes to the surface. For latent heat, a positive flux signifies evaporation, while a negative flux signifies condensation – for open water, the flux is usually positive. For sensible heat, a positive flux signals that the water is heating the overlying air (daytime), and vice versa for a negative flux (nighttime). The fluxes occur simultaneously and can be considered as a single process. This means that they are calculated by similar methods, the generic approach is that the flow rate is equal to the concentration of the difference divided by the resistance to flow. It can further be assumed that the aerodynamic resistance to flow for water vapour and heat transport are the same. For open water, around 90 per cent of the net allwave radiation absorbed by the water is used for evaporation and the Bowen ratio (sensible : latent heat) is low; around 0.2 on a long-term basis for shallow water (Oke, 1987). The predominance of positive latent heat fluxes from open water has a cooling effect on the water body and overlying air.

In the turbulent heat flux sub-model, the latent heat and associated water losses are calculated separately for open water and vegetation using variations of the combination method.

The sub-model inputs and parameters are given in Tables 4 and 5, outputs are the volumes of evaporation and evapotranspiration from the open water surface and the vegetation canopy respectively (m³/h). Given that wetlands tend to be shallow (TP 10 suggests around 1 m depth), the turbulent heat flux sub-model is lumped. It is assumed that the vegetation has an unbroken canopy which covers the water surface below the plantings and that water in the open water permanent pools is fully mixed with no temperature stratification. The convention is that positive fluxes are from the surface (ie, result in evaporation) while negative fluxes to the surface (ie, condensation).

4.3.1 Water temperature

Knowing the water temperature of the wetland is essential for the calculation of not only the turbulent heat fluxes, but also longwave radiation from the water surface (equation 28 above). A water depth of 1.5 m requires almost 2000 W/m² to change water temperature by 1°C. Here it is assumed that change in water temperature with each timestep is a function of the water depth and energy availability ΔQ_s (equation 2) and that there is neither stratification nor horizontal gradients. In reality, water surface temperature will vary between points as a result of spatial differences in water depth, energy availability and mixing (ie, the combined effects of convection, wind currents and flow patterns causing local advection). Moreover, vertical stratification driven by density differences can develop. The change in temperature for the open water pools is calculated as:

$$\frac{\Delta T_w}{\Delta t} = \frac{\Delta Q_s}{z_w \rho_w C_w} \quad \text{Equation 33}$$

Where z_w is the water depth (equated to the average depth of the open water pools), ρ_w is water density, C_w is the specific heat of the water and t is time. Water density is calculated from the empirical relationship:

$$\rho_w = 1000 \left(1 - \frac{T_w + 288.9414}{108929.2 T_w + 68.12963 T_w^2 - 3.9863 T_w^3} \right) \quad \text{Equation 34}$$

Water temperature is given a lower limit of 0°C and ice formation and melt are not simulated. In cooler regions, ice can be modelled using a degree-day empirical method, however, in Auckland's temperate climate, an ice routine is not warranted.

Table 4

Inputs for the turbulent heat flux sub-model .

| Input | Symbol | Unit | Source |
|----------------------------------------------------------|----------|------------------|----------------------------------------------------------------------------------------------------------------------------------------------------------------------------------|
| Air temperature | T_a | °C | Input.xls |
| Vegetation temperature | T_v | °C | Assumed equal to T_a |
| Net allwave radiation for vegetation | Q_v^* | W/m ² | Radiation.xls |
| Net allwave radiation for water | Q_w^* | W/m ² | Radiation.xls |
| Saturated air vapour pressure | e_o | Pa | Input.xls |
| Actual air vapour pressure | e_a | Pa | Input.xls |
| Saturated vapour pressure over water | e_w | Pa | Calculated as: $e_w = 610.8e^{\left(\frac{17.27T_w}{T_w+237.3}\right)}$ Equation 35 |
| Psychrometric constant | γ | Pa/°C | Calculated as: $\gamma = 0.66 \frac{e_o}{T_a} + 0.00115 T_a \bar{P}_o$ Equation 36 Where \bar{P}_o is atmospheric pressure as a function of site elevation (equation 36) |
| Slope of saturation vapour density VS. temperature curve | δ | Pa/°C | Calculated as: $\delta = \frac{4098e_o}{T_a + 237.3}$ Equation 37 |
| Wind speed | u | m/s | Input.xls |
| Volume water stored in wetland | S | m ³ | Flow.xls |
| Open water surface area | A_w | m ² | Flow.xls |

Table 5

Parameters for the turbulent heat flux sub-model.

| Parameter | Symbol | Value | Unit | Input status |
|-----------------------------------------------------------------------|---------------------|----------|-------------------|-------------------------------------------------------------------------------------------------------|
| Timestep | t | Variable | s | Flow.xls |
| Elevation above sea level | masl | Variable | m | User defined |
| Atmospheric pressure | P_o | Variable | Pa | Calculated as: $P_o = 101.3 \left(\frac{293 - .0065 \text{masl}}{293} \right)^{5.26}$ Equation 38 |
| Density of air | ρ | 1.2 | kg/m ³ | Unchangeable |
| Heat capacity of air | C_a | 1013 | J/kg/K | Unchangeable |
| Heat capacity of water | C_w | 4180 | J/kg/K | Unchangeable |
| Von Karman's constant | k | 0.4 | - | Unchangeable |
| Height of instruments | z | Variable | m | User defined (2 m standard) |
| Emergent vegetation height | z_v | Variable | m | User defined |
| Zero plane displacement for vegetation | d_v | Variable | m | Calculated as: $d_v = \frac{3}{4} z_v$ Equation 39 |
| Roughness length for vegetation governing transfer of momentum | z_{om} | 0.072 | m | Unchangeable |
| Roughness length for vegetation governing transfer of heat and vapour | z_{oh} | Variable | m | Calculated as: $z_{oh} = \frac{z_{om}}{10}$ Equation 40 |
| Stomatal resistance of wetland vegetation (wet) | $r_{s,wet}$ | Variable | s/m | User defined (default 0) |
| Stomatal resistance of wetland vegetation (dry) | $r_{s,dry}$ | Variable | s/m | User defined (default 70) |
| Threshold water storage | S_w | Variable | m ³ | User defined |
| Roughness length for water | z_{ow} | 0.00137 | m | Unchangeable |
| Ratio of open water to vegetation | Ratio _{wv} | Variable | | Flow.xls |
| Area of emergent vegetation at overflow | A_v | Variable | M ² | Flow.xls |
| Height to invert level | h_o | Variable | m | Flow.xls |

4.3.2 Latent heat, evaporation and evapotranspiration

Evapotranspiration is the composite of water losses from the land surface to the atmosphere and is equated to the latent heat flux divided by the latent heat of vaporization. Evapotranspiration from a wetland has a number of sources and pathways, evaporation from bare soil at the wetland margins and free water (either free water on vegetation or open water in the water pools), and transpiration from vegetation (ie, through stomata). Water balance calculations for vegetated surfaces make a distinction between potential (PET) and actual (AET) evapotranspiration rates. PET is defined as the maximum amount of water that would evaporate or transpire given the prevailing climate from a short green crop completely covering the soil surface if water were not limited. In contrast, AET is the amount of water that is lost and is a function of water availability, usually expressed in terms of soil moisture storage, and plant physiology (expressed as aerodynamic resistance of the stomata to water loss).

4.3.2.1 Open water

The latent heat flux for open water is calculated using the Penman (1948) method:

$$Q_{EW} = \frac{1}{\delta + \gamma} \left[\delta (Q_w^* - Q_A) + \left(\frac{C_a (e_w - e_a)}{r_{aVap}} \right) \right] \quad \text{Equation 41}$$

Where δ is the slope of the saturated vapour density versus air temperature curve (equation 35), γ is the psychrometric constant (the ratio of specific heat of moist air at constant pressure to the latent heat of vaporisation, equation 34), C_a is the heat capacity of air, e_w is the saturated vapour pressure above the water surface (equation 33), e_a is the vapour pressure of the air (equation 4) and r_{aVap} is the aerodynamic resistance to flow for water vapour. Under the assumption that the resistance to flow for water vapour is the same as that for heat transfer (r_{aH}), r_{aVap} can be calculated using a bulk aerodynamic approach as:

$$r_{aVap} = r_{aH} = \frac{\left(\ln \left[\frac{z}{z_w} \right] \right)^2}{k^2 u} \quad \text{Equation 42}$$

Where z is the height of the wind measurements, z_w is the roughness length for calm water (ie, where wind speed = zero under the assumption of a logarithmic wind profile) and is set to 0.00137 m (Shuttleworth, 1992), k is Von Karman's constant and u is wind speed.

The volume of evaporation from the open water surface is then calculated as:

$$E_w = \frac{Q_{EW}}{L_w} A_w \quad \text{Equation 43}$$

Where A_w is the surface area of the open water (which varies according to equation 57), L_w is the latent heat of vaporization at the water temperature T_w which can be calculated using the empirical relationship :

$$L_w = 10^6 (10^{-5} T_w^2 - 0.00260 T_w + 2.5009) \quad \text{Equation 44}$$

4.3.2.2 Vegetation

The model makes the assumption that the soil surrounding the wetland is saturated in order to simplify calculation and avoid spurious accuracy. This means that the water balance does not need a soil moisture sub-routine and AET is equated to PET until the wetland is empty after which, AET=0. For a shallow wetland with a permanent wet pool and vegetated margins where water is not limited, the assumption is valid under normal operational conditions. If there is no aerodynamic resistance, AET from the vegetation can be equated to evaporation from open water, however, as vegetated surfaces do have some resistance to water loss through stomata, the two can differ. Generally, PET increases and resistance of plants to drying decreases with increasing water status (Lafleur *et al.*, 1992; Eugster *et al.*, 2000), thus in a wetland, the difference between open water evaporation and PET from the vegetated surfaces is likely to be minimal given the same energy inputs.

The model uses the Penman-Monteith (Monteith, 1965, 1981, 1985) method to determine PET for the wetland vegetation:

$$Q_{EV} = \frac{1}{\delta + \gamma} \left[\frac{\delta Q_v^* + \frac{C_a (e_o - e_a)}{r_{aVV}}}{1 + \frac{r_s}{r_{aVV}}} \right]$$

Equation 45

Where r_s is the stomatal resistance of the plants to transpiration and r_{aVV} is the aerodynamic resistance of flow for water vapour from the vegetation.

The main difficulty of applying the Penman-Monteith formula to wetlands is the choice of the resistance parameters. In a study of natural wetlands in the UK which compared calculated estimates of PET for nearby agricultural land against measurements made using eddy correlation for a reed bed and a grassed wetland, Acreman *et al.* (2003) found that the reed bed wetland had evaporative losses some 14 per cent greater than the grassed wetland and both had PET significantly higher than the regional Penman estimates. They found that the Penman estimates were only valid for the wetlands during high summer when the water table dropped below the soil surface. Acreman *et al.* (2003) used the eddy correlation data to estimate values for stomatal resistance and found a wide spread. However, there were two clear trends: when water was limiting as the wetland dried in summer, the resistance approached 70 s/m, which is the FAO recommended resistance for grasses (Allen *et al.*, 1998);

when water was freely available, the resistance scattered around zero. For the latter case, resistance ranged from -250 s/m (ie greater PET than open water evaporation) to as much as 500 s/m. This finding reflects that fact that the vegetation has greater exposure to drying winds than the water surface and transpire freely through the stomata.

The model has two stomatal resistance parameters – wet and dry - the choice of which is a function of water storage in the wetland. If the wetland has full storage, the resistance is set to zero. If the storage drops below a user defined threshold, S_T , the resistance is set to 70 s/m. For Longford Park, the rushes are planted on submerged ridges with their roots below invert level but above the permanent pool base. The default threshold storage (1500 m³) is equivalent to the storage held up to the planting level in the three open water pools. For Wainoni Wetland 2, the vegetation is planted on the wetland base, thus the default threshold water storage is zero.

The bulk aerodynamic resistance term is similar to equation 43 and is calculated as:

$$r_{aVV} = \frac{\ln\left[\frac{z-d}{z_{oh}}\right] \ln\left[\frac{z-d}{z_{om}}\right]}{k^2 u} \quad \text{Equation 46}$$

Where d is the zero displacement plane (equation 37), z_{oh} is the vegetation roughness length governing transfer of heat and vapour (0.072 for wetland reeds and rushes according to Acreman *et al.*, 2003) and z_{om} is the roughness length governing the transfer of momentum (equation 38). Note that at Longford Park, the emergent wetland vegetation responsible for evapotranspiration is also that which shades the water and $H_v = z_v$, however, at Wainoni Wetland 2, the marginal vegetation is responsible for shading while the emergent vegetation is responsible for evapotranspiration.

The volume of evapotranspiration from the vegetation is then calculated as:

$$PET_V = \frac{Q_{EV}}{L_v} A_v \quad \text{Equation 47}$$

Where A_v is the vegetated surface area of the wetland, L_v is the latent heat of vaporization at the temperature of the vegetation (assumed to be same as air temperature) which is calculated using the empirical relationship :

$$L_v = 10^6 (10^{-5} T_a^2 - 0.00260 T_a + 2.5009) \quad \text{Equation 48}$$

4.3.3 Sensible heat

Sensible heat is calculated here for the water surface in order to simulate the water temperature. The model uses a bulk aerodynamic method which requires wind speed at only one height (Oke, 1987). This method is only suitable for stable conditions and is written as:

$$Q_{HW} = \frac{C_a (T_w - T_a)}{r_{aH}}$$

Equation 49

Where r_{aH} is the aerodynamic resistance to heat transfer over water calculated as above (equation 43) according to the assumption that the resistance is similar to that for the transfer of water vapour.

4.4 Flow sub-model (Flow.xls)

The flow sub-model solves the wetland water balance according to equation 1. Outflow is determined as a function of the hydraulic head above invert level of the outlet structure which is itself a function of water volume and wetland layout and size. No attempt has been made to simulate flow paths through the wetlands and it is assumed that there is plug flow with water able to move unhindered from inlet to outlet. For Wainoni Wetland 2, this assumption is justified as the wetland consists of a single pool planted with emergent vegetation (though there could be some localised dead areas and preferential flow due to the vegetation). However, at Longford Park, the rushes are planted on submerged ridges and there are three separate water pools. Under normal wet conditions, the water level is above the ridges and the pools are linked and have the same water level (the invert level when at full storage), however under very dry conditions when the water level drops below 0.3 m from the invert, the vegetation ridges could act as barriers to flow. The input data and parameters are the same for both wetlands and are given in Tables 6 and 7. Output is the outflow from the wetland.

Table 6

Inputs for the flow sub-model.

| Input | Symbol | Unit | Source |
|------------------------------------|----------|-------------------|----------------------|
| Inflow | F_{in} | m ³ /h | Input.xls |
| Evaporation from open water | E_w | m ³ /h | Turbulent fluxes.xls |
| Evapotranspiration from vegetation | PET_v | m ³ /h | Turbulent fluxes.xls |

The default parameters for both wetland outlets have been taken from design and maintenance documentation supplied to the ARC as described above.

For each wetland, the initial storage is set to the storage volume at overflow (ie, the storage when the water level is the same as the outlet invert level), thereafter, storage at each timestep (t) is calculated as:

$$S_{(t)} = S_{(t-1)} + F_{in} - PET_v - ET_w - F_{out}$$

Equation 50

Hydraulic head is calculated by solving the quadratic equation below for a trapezoid basin. This equation describes the basin dimensions above the invert level:

$$H = 0$$

$$S \leq S_o$$

$$H = \frac{-W_o L + \sqrt{W_o^2 L^2 - 4\Delta L (S - S_o)}}{2\Delta}$$

$$S > S_o$$

Equation 51

Where W_o is the average width of the wetland basin at overflow, L is the length of the wetland and Δ is the trapezoid slope (expressed as bank width to bank height).

Table 7

Parameters for the flow sub-model .

| Parameter | Symbol | Value | Unit | Input status |
|------------------------------------------------------|-----------------------|----------|----------------|----------------------------------------------------------------------------------|
| Timestep | t | Variable | s | User defined |
| Wetland surface area at overflow | A_o | Variable | m ² | User defined |
| Area of open water at overflow | A_{wo} | Variable | m ² | User defined |
| Area of emergent vegetation at overflow | A_v | Variable | m ² | Calculated as: $A_v = A_o R_v$ Equation 52 |
| Ratio of water to wetland surface area | R_w | Variable | | Calculated as: $R_w = \frac{A_w}{A_o}$ Equation 53 |
| Ratio of emergent vegetation to wetland surface area | R_v | Variable | | Calculated as: $R_v = 1 - R_w$ Equation 54 |
| Storage volume at overflow | S_o | Variable | m ³ | User defined |
| Total flow length | L | Variable | m | User defined |
| Invert level of the outlet | h_o | Variable | m | User defined |
| Slope (width to height ratio) | Δ | Variable | | User defined |
| Width of wetland at overflow | W_o | Variable | m | User defined |
| Acceleration due to gravity | g | 9.8 | m/s | Unchangeable |
| Width of the weir crest | W_c | Variable | m | User defined at Longford Park Calculated with equation 58 at Wainoi Wetland 2 |
| Standpipe diameter | | Variable | m | User defined (Longford Park) |
| Weir coefficient Broad-crested | Cd_{BROAD} | Variable | | User defined (Longford Park) |
| Orifice coefficient | Cd_{ORIFICE} | Variable | | User defined (Wainoni Wetland 2) |
| Weir coefficient Sharp-crested | Cd_{SHARP} | Variable | | User defined (Wainoni Wetland 2) |
| Number of contractions | i | Variable | | User defined (Wainoni Wetland 2) |

Outflow at Longford Park is calculated with the standard discharge equation for a broad crested transverse weir:

$$F_{out} = 0 \quad H = 0$$

$$F_{out} = Cd_{BROAD} \frac{2}{3} W_c \sqrt{2g} H^{\frac{3}{2}} \quad H > 0 \quad \text{Equation 55}$$

Where Cd_{BROAD} is the weir coefficient for a broad-crested weir, W_c is the width of the weir crest and g is acceleration due to gravity. A coefficient of 0.6 is a fairly typical upper value for broad-crested weirs (Butler and Davies, 2001). Simulated outflow is very sensitive to the choice of coefficient, the higher the value, the less the detention period and the greater the outflow peaks. Whether the simulation is correct cannot be determined without calibration. The default weir coefficient for Longford Park is 0.4, this value gives roughly a two-hour detention time and some flow attenuation.

The flow situation at Wainoni Wetland 2, where outflow is via a 1.8 m diameter standpipe, is more complex than at Longford Park and equation 56 cannot be used. Akan and Houghtalen (2003) state that flow from standpipes is not well documented. Structures such as grates and anti-vortex devices further complicate the hydraulics of standpipes, and the flow from Wainoni Wetland 2 may be restricted by its debris screen which consists of 30 bars of around 2 cm diameter arranged around the rim. Apart from reducing the length of the crest, the bars could cause side contraction.

For most flow conditions, a standpipe can be expected to act as a sharp-crested weir, however, if the water level completely covers the standpipe, the outlet could behave as an orifice. The transition from weir to orifice flow is indistinct, a rule-of-thumb is when the hydraulic head is equivalent to the standpipe radius. As the size of the outlet at Wainoni Wetland 2 compared to the wetland storage is fairly large, it is unlikely that orifice flow would develop. Even so, outflow in equation 57 below is calculated both with the sharp-crested weir (with contraction) and orifice formulae and outflow is said to be the minimum of these.

$$F_{out} = 0 \quad H = 0$$

$$F_{out} = \min \{ F_{outSHARP} : F_{outORIFICE} \} \quad H > 0$$

$$F_{outSHARP} = Cd_{SHARP} \frac{2}{3} W_c - 0.1iH \sqrt{2g} H^{\frac{3}{2}}$$

$$F_{outORIFICE} = Cd_{ORIFICE} A_{ORIFICE} \sqrt{2gH} \quad \text{Equation 56}$$

Where i is the number of contractions (ie, 30 bars), and $A_{ORIFICE}$ is the area of the standpipe opening.

The width of the crest and the area for the standpipe are calculated as:

$$W_c = 2\pi \text{radius} \cdot i \text{width of bars} \quad \text{Equation 57}$$

$$A_{ORIFICE} = \pi \text{radius}^2 \quad \text{Equation 58}$$

The coefficient for an orifice range to reflect ragged and square edges respectively (US National Highway Institute, 2001). The choice of coefficient is not clear cut for standpipes and there are no widely accepted values (Akan and Houghtalan, 2003). The US National Highway Institute (2001) gives a range of values for broad-crested weirs related to width and hydraulic head and suggest a value of around 0.49 for a weir with an equivalent width (4 m) and a head of 0.1 – 1.6 m. Sharp-crested weirs generally have similar coefficients. However, the debris screen and emergent vegetation mean that the coefficient is probably less, the value chosen here is 0.1.

The surface areas for the open water and vegetated surfaces are calculated in the flow sub-model as they are functions of the wetland dimensions and, in the case of open water, hydraulic head. These variables are used in the turbulent fluxes sub model to simulate ET_w and PET_v . The vegetated area is assumed to be constant and is calculated using equation 51 above, water surface area is calculated as:

$$A_w = L W_o + 2\Delta H \quad A_v \quad \text{Equation 59}$$

5 Results with Discussion

For each wetland, there are two sets of model runs – with and without emergent and marginal vegetation – to simulate the effects of vegetation on both flow and water temperature. In the absence of vegetation, both wetlands can be equated to wet detention ponds thus allowing some comparison between ponds and wetlands that can be used to indicate the relative importance of vegetation on flow reduction and attenuation. Vegetation was removed from the model by simply changing the vegetation cover ratio and the vegetation height to zero. In the case of Longford Park, the original pond dimensions (ie, no submerged ridges and even depth of 1.5 m) were used in the pond simulations.

It must be stressed that the model has not been calibrated due to the absence of monitoring at both sites. The following results and discussion make the assumption that the simulations are realistic.

5.1 Radiation

The global solar radiation calculated in the model for the situation where there is no shading or loss of sky-view can be compared to those observed at the NIWA monitoring station at Auckland Airport. The examples given below are for summer and winter conditions at Longford Park (Figures 10 and 11), the correlation for the entire simulation period is $R^2=0.86$. The model tends to slightly underestimate solar radiation under sunny conditions and overestimate under cloudy conditions.

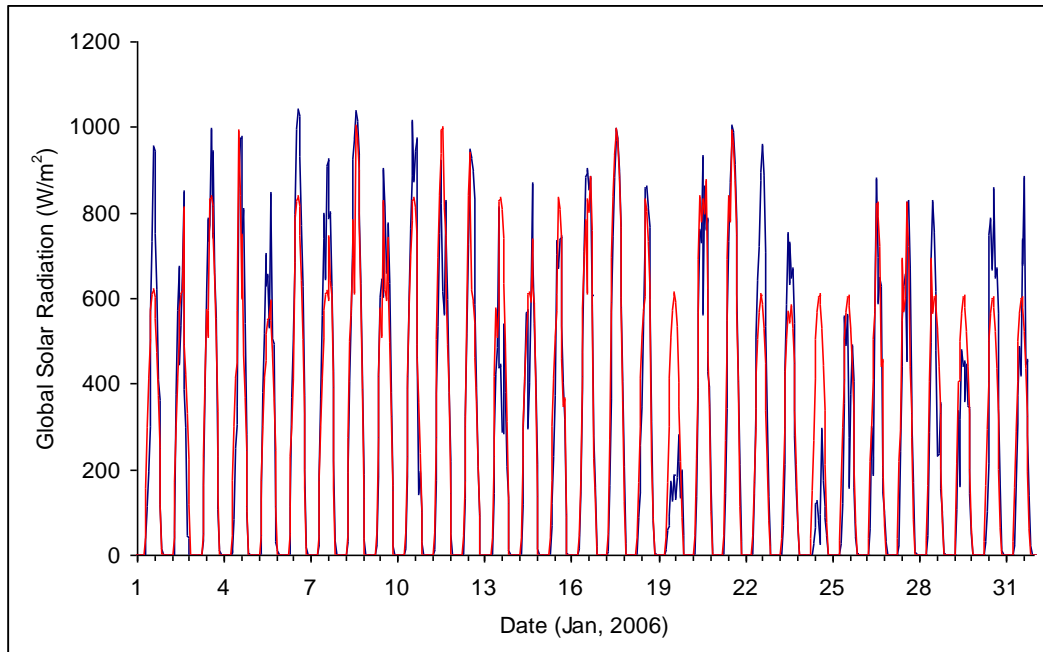
5.1.1 Longford Park

Radiation reaching the water surface is modified by vegetation. Direct solar radiation is reduced due to shading by emergent vegetation and both incoming longwave and diffuse solar radiation are limited by the sky-view. On the other hand, longwave radiation emitted by the open water is greater than for the vegetation (recall the emissivity of water is higher than the emissivity of vegetation) and does not show the same diurnal variability because of the assumption that vegetation has the same temperature as the air whereas water temperature is less variable. Figure 12 shows net allwave radiation at Longford Park. The net allwave radiation available to the vegetation is greater (around 40 W/m^2) than for the water surface with the exception of the hours around noon, particularly in summer, when the sun is high in the sky. At that time water has its lowest albedo (reflection), the effect of shading is least and the radiation available to the open water at Longford Park is some 19 W/m^2 greater than for the vegetation.

Figure 10

Observed (blue) and calculated (red) global incoming solar radiation for a. summer (January 2006) and b. winter conditions (July, 2006).

a.



b.

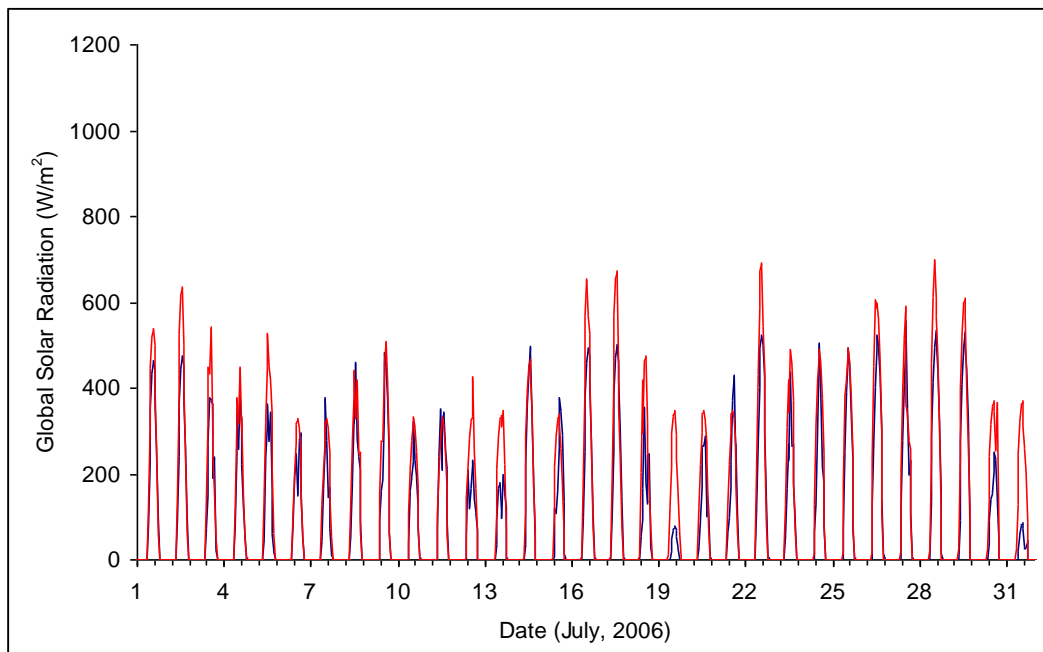


Figure 11

Observed vs. simulated global radiation showing linear regression line and equation. The 1:1 line is also given (dashed cerise).

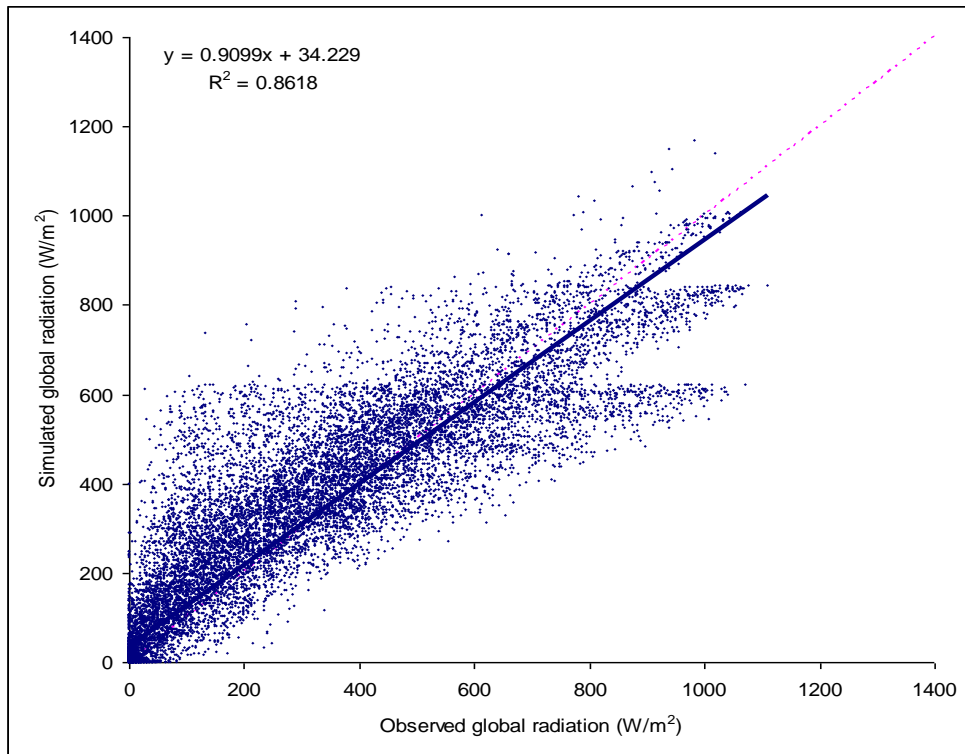
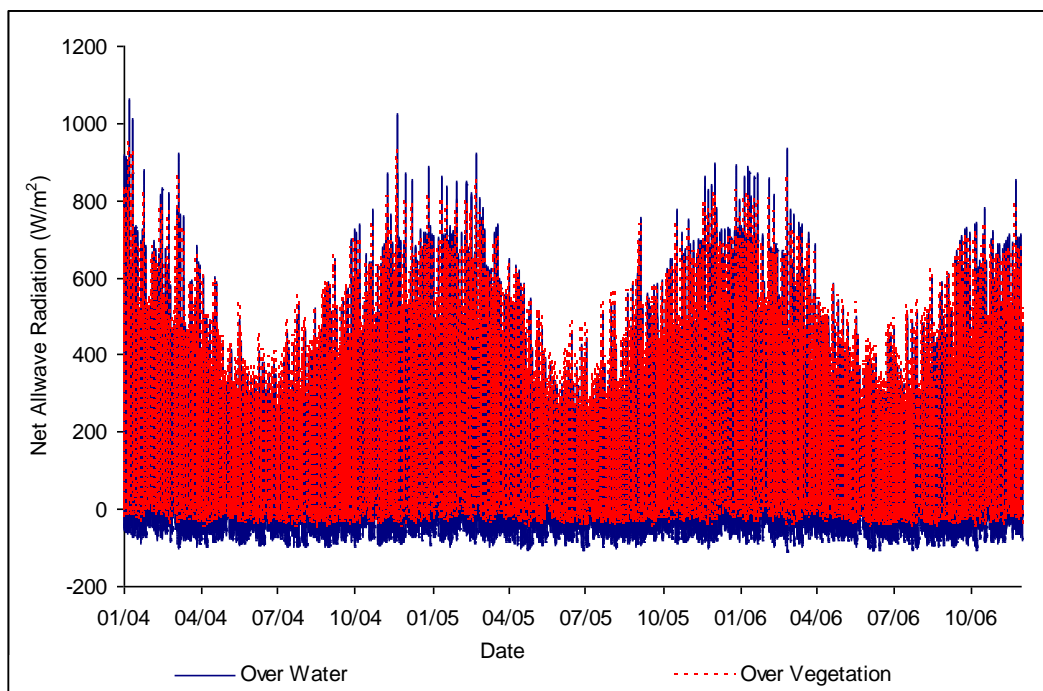


Figure 12

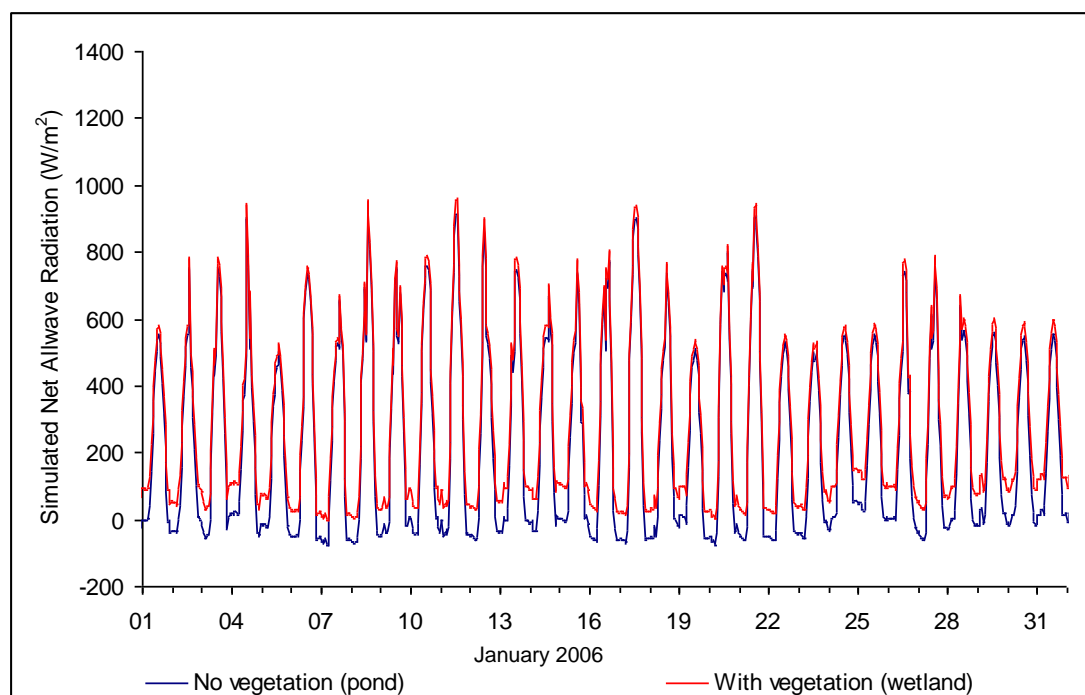
Simulated net allwave radiation for Longford Park.



The effect of emergent vegetation on shading is very small during the daytime due to the low height of the reeds (particularly during the middle of the day when the sun is high in the sky) compared to the width of the open water pools. On average, vegetation slightly decreases the net allwave radiation reaching the water surface (Figure 13). On the other hand, at night the pond simulation has greater longwave emissions than the emergent vegetation due to the warmer water (see below).

Figure 13

Simulated net allwave radiation over open water for Longford Park showing the effect of emergent vegetation, January 2006.

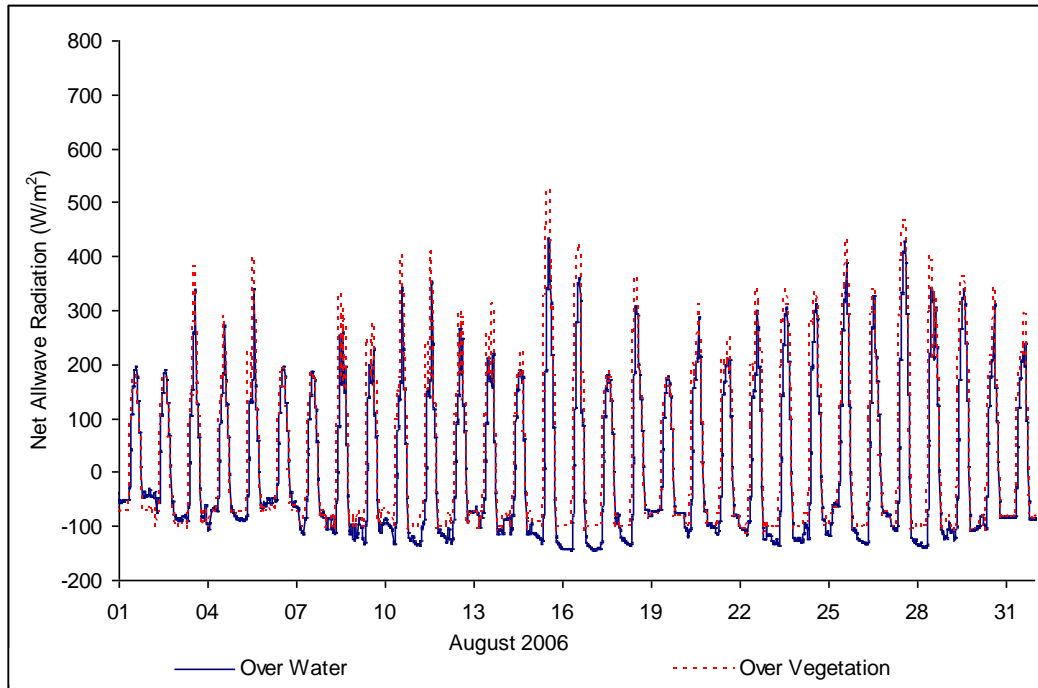


5.1.2 Wainoni Wetland 2

Unlike Longford Park, Wainoni Wetland is small and narrow with low emergent vegetation covering much of the wetland surface. The wetland is surrounded by native shrubs with varying heights of up to 2 m. The canopy is less dense than base, an effective “average” height of 1.5 was chosen as the default. The bank vegetation both shades the wetland from direct solar radiation and reduces sky-view (incoming longwave and diffuse shortwave radiation). The emergent vegetation and water surface are both shaded by the bank vegetation and have the same incoming allwave radiation. The net allwave radiation differs slightly (Figure 14) due to different surface albedos and emissivities. The water surface is likely to have greater radiative cooling than at Longford Park (ie, incoming longwave radiation is consistently less than outgoing longwave emitted due to the reduced sky-view).

Figure 14

Simulated net allwave radiation over open water and emergent vegetation Wainoni Wetland 2, August 2006.



5.2 Water temperature

The model simulates bulk or average water temperature assuming that there is both total horizontal and vertical mixing. Obviously, water under or close to emergent vegetation or which is shaded by the wetland banks will be cooler than water that is fully exposed to the sun. Moreover, shallow water will heat more rapidly than deep water. Some thermal stratification could occur as the upper water layers heat up during the day, becoming less dense, and cool at night. To simulate horizontal and vertical temperature gradients would require full hydraulic simulation of the wetlands and is outside the scope of this project.

5.2.1 Longford Park

For Longford Park, the simulations show that the wetland tends to store heat during the day for release at night. Water has a greater heat capacity than air, this means that it takes more energy to heat up and retains heat longer. Hence it is not surprising that the simulated water temperature smoothes out the diurnal fluctuations in air temperature seen at both wetlands (Figure 15). Indeed, a comparison of average daily air temperature against average daily water temperature for Longford park shows a strong relationship ($R^2=0.84$). There is a lag between the daily air and water temperature of one to three days depending on the weather conditions. The simulated

water temperature is generally warmer than air, the mean difference for the daily average is around 2°C but can be up to 7°C. There is no seasonality in the difference between air and water temperature.

There is only a small difference between the bulk water temperature modelled with and without emergent vegetation (Figure 16) – the wetland has a bulk temperature around 1° cooler than the pond due to shading and reduced sky-view. As stated above, the water close to the banks and vegetated ridges could be cooler due to the shading and reduction of sky-view. Running the model with different depths showed that the water temperature is more sensitive to water depth than the presence of emergent vegetation with the water heating and cooling more rapidly.

5.2.2 Wainoni Wetland 2

The situation at Wainoni Wetland 2 is quite different from Longford Park due to the effect of shading and reduced sky-view of both the emergent vegetation and the open water surface caused by bank vegetation. As at Longford Park there is smoothing of the diurnal air temperature fluctuation. The wetland is only 50 cm deep on average, hence the water's response to radiation is more rapid. Figure 17 suggests that the simulated water temperature is cooler than air temperature in winter and warmer in summer. During spring, water temperature seems to track the daily average air temperature. The seasonal differences in water temperature with respect to air temperature can be largely explained by shading by the bank vegetation. In winter when the sun elevation is lower, shadows cast by the bank vegetation will be longer reducing incoming solar radiation. This coupled with the greater albedo with low sun angles means that the wetland remains cool during the winter months. In summer, the sun elevation is higher and the wetland is more exposed to incoming solar radiation so that the water quickly heats up and remains warmer than the ambient air temperature.

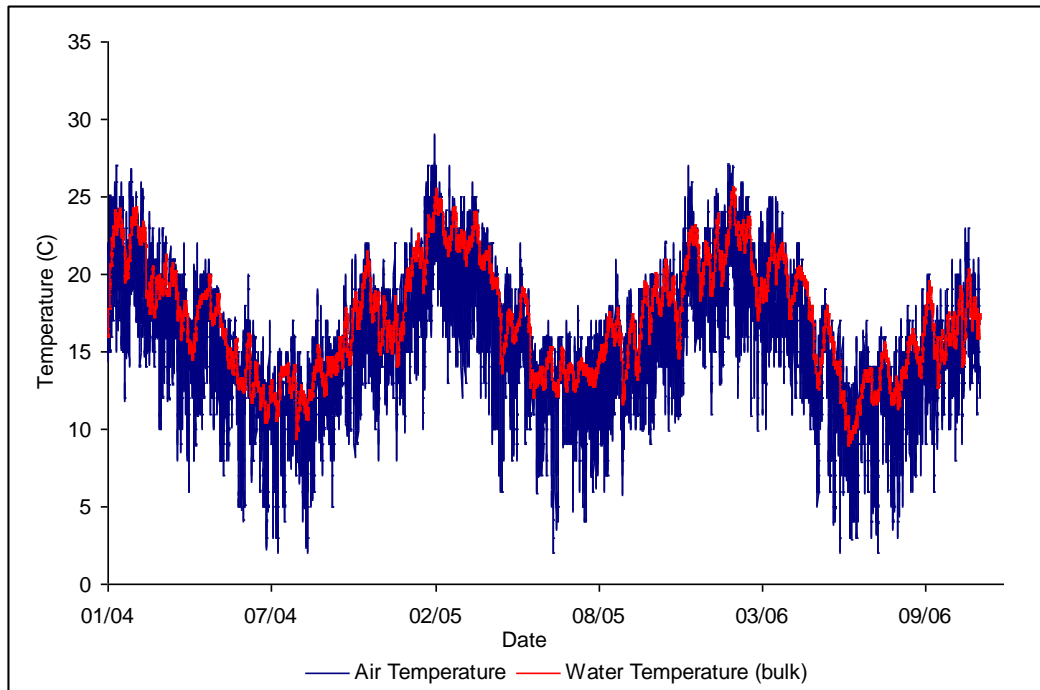
It should be noted that the temperature sub-model is very sensitive to the height of the bank vegetation which governs shading and sky-view. Increasing the height cools the wetland while decreasing the height warms the wetland. The seasonal differences remain in both cases. Hence, bank vegetation could offer a means of cooling small shallow wetlands to improve summer water quality.

Removing the emergent vegetation has a negligible impact on simulated bulk water temperature.

Figure 15

Observed air temperature against water temperature simulations for Longford Park: a. hourly (2004-2006); b. daily averages (2004).

a.



b.

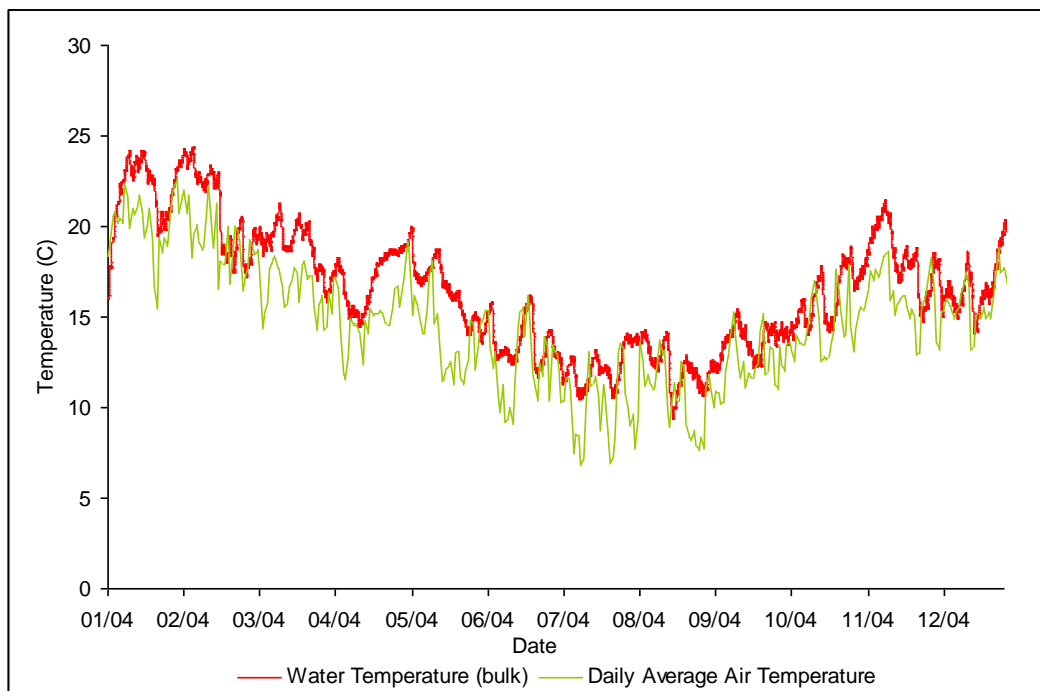


Figure 16

Simulated bulk water temperature at Longford Park (2006) showing the effect of emergent vegetation – ie, pond vs. wetland model parameters.

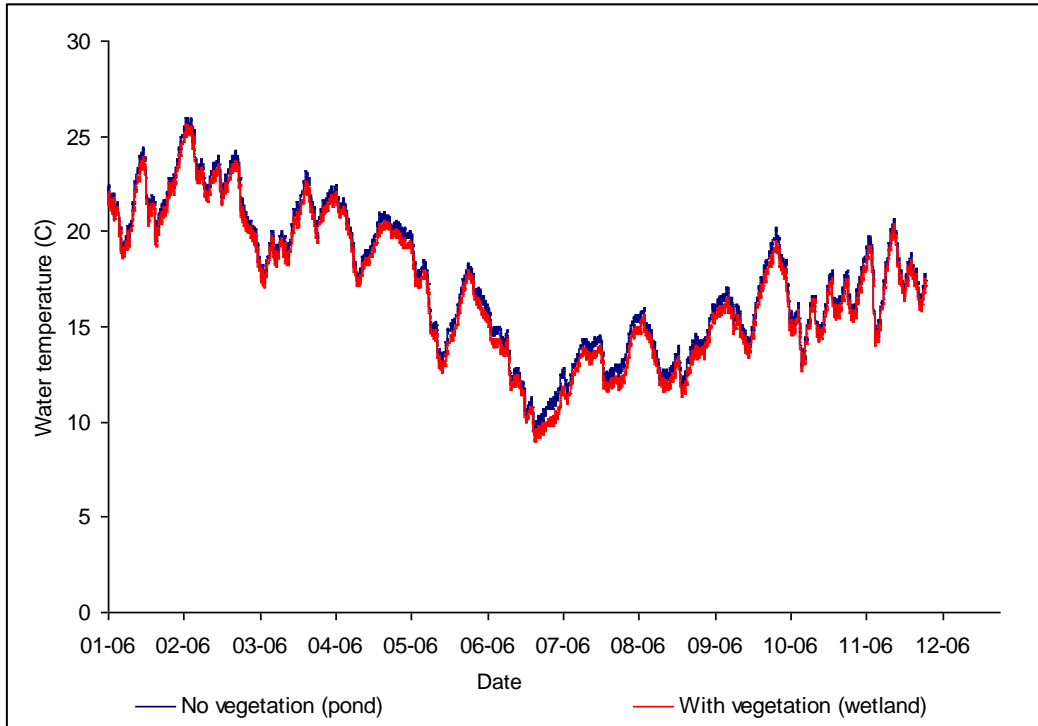
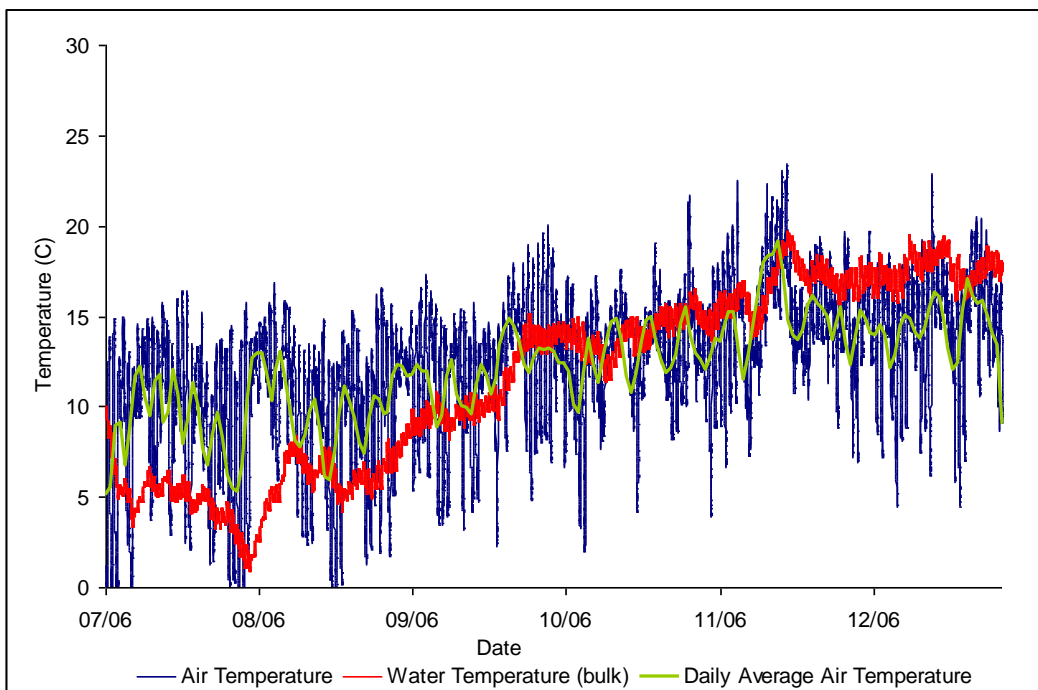


Figure 17

Observed air temperature against water temperature simulations for Wainoni Wetland 2.



5.3 Turbulent fluxes and evapotranspiration

For both wetlands under baseflow (dry weather) conditions, the latent heat over the emergent vegetation is greater than over open water. This is largely due to the greater exposure of the emergent vegetation to wind and incoming radiation. The effect is more pronounced at Longford Park where the reeds are not shaded by riparian shrubs and reach a height of some 1.2 m above the water. Wind is therefore able to blow through the reeds which have a greater surface area for evapotranspiration than the horizontal water surface. It should also be noted that the wetland plants have a lower albedo on average than water which means they are able to absorb more solar energy – one of the main drivers of evapotranspiration.

As mentioned above, the Bowen ratio for open water is low, which means that the sensible heat flux is minor compared to latent heat. The sensible heat flux over water fluctuates around zero; positive fluxes are from the water surface while negative fluxes to the surface. A positive flux signals that the water is heating the overlying air (daytime), and vice versa for a negative flux (nighttime). In general, open water has a cooling effect on the air. In fact, the ability of water to cool is the principal behind the Mediterranean idea of courtyard fountains.

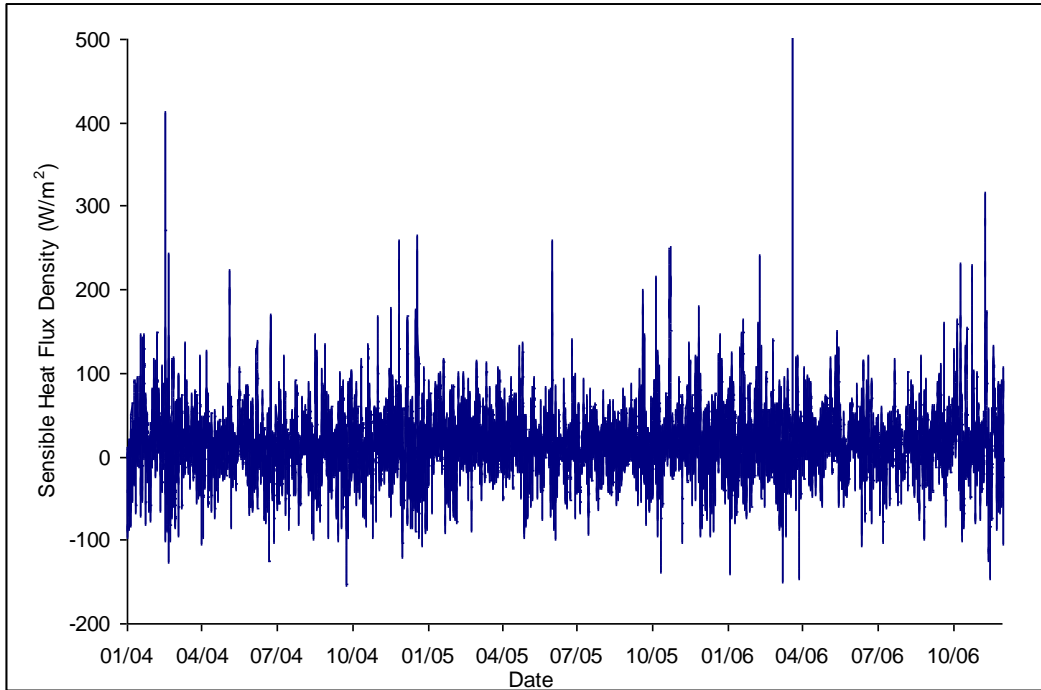
5.3.1 Longford Park

Figure 18 Shows the turbulent fluxes at Longford Park. Figure 18a shows that sensible heat fluctuates around zero and has a diurnal cycle. As can be expected, the latent heat flux is much greater than sensible heat and the Bowen ratio is around 0.36 on average (median value is 0.19). Figure 18b suggests that the vegetation has a greater latent heat flux than open water which suggests the vegetation can increase wetland water loss. This is partly because the vegetation has a greater surface exposure to the air (and wind) compared to water. However, the turbulent flux sub-model is sensitive to the choice of stomatal resistance. The default value is zero s/m when there is unlimited water and 70 s/m (ie, same as grass) when the wetland dries on the basis of research in the UK. Acreman *et al.* (2003) found that wetland plants typically have low stomatal resistance to drying, this coupled with the greater surface area (and therefore exposure to wind) compared to the water means that the latent heat flux can be greater than over water. However, they do note that there is a wide spread of resistances. If a stomatal resistance of a credible 25 s/m is used in the model instead, the latent heat fluxes for vegetation and water become virtually indistinguishable. A resistance of 50 s/m leads to greater simulated latent heat over water than vegetation. The simulated latent heat flux over both vegetation and water in Figure 18b is generally positive (evapotranspiration), though there can be some negative values at night (condensation) albeit slight.

Figure 18

Turbulent heat fluxes at Longford Park Wetland: a. sensible heat over open water; b. latent heat over vegetation and open water.

a.



b.

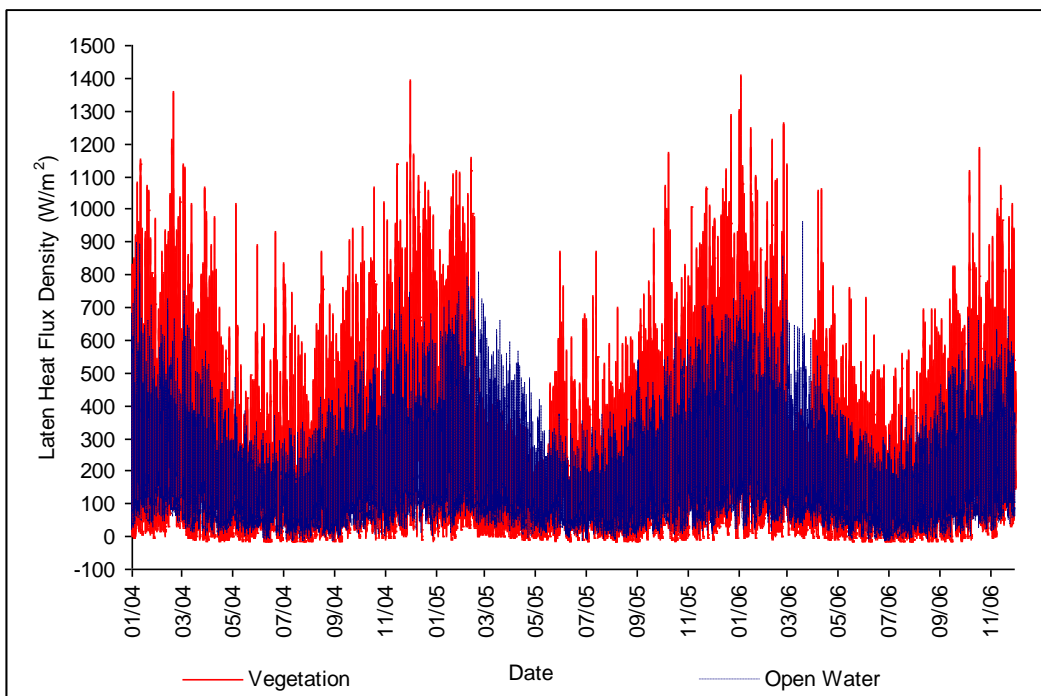
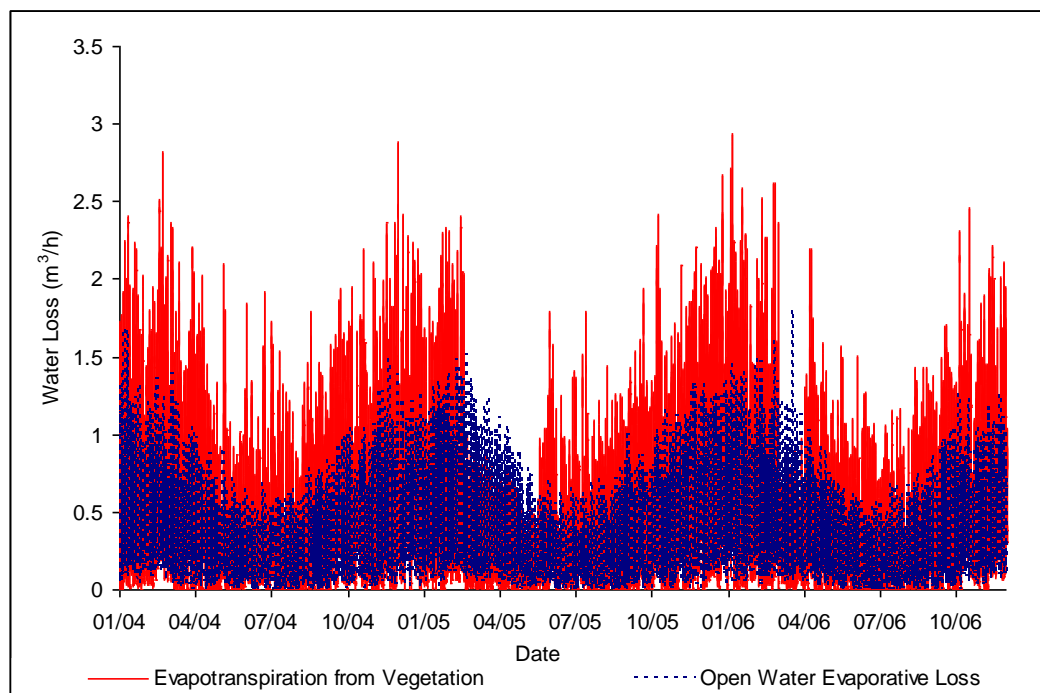


Figure 19 shows the volume of evapotranspiration from each surface respectively. The volume is a function of the areas covered by open water and vegetation as well as the latent heat flux. The simulated evapotranspiration from the emergent vegetation is greater than the evaporative losses from open water. The difference can be up to 6 mm per day for each surface.

Figure 19

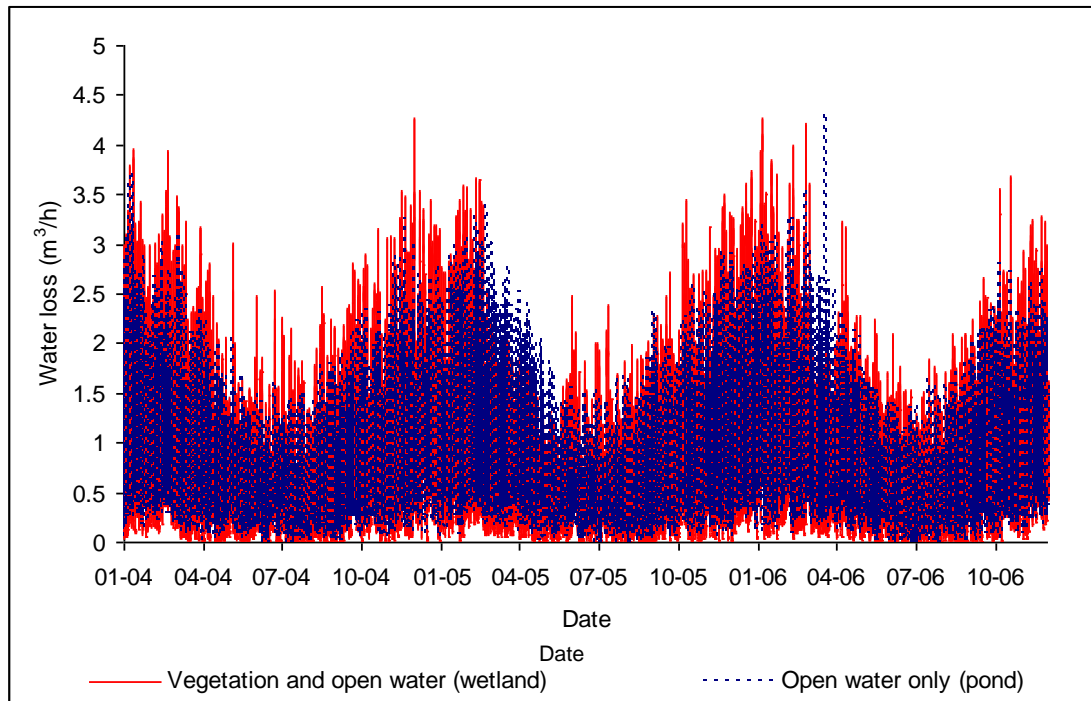
Evaporation and evapotranspiration from the different surfaces at Longford Park Wetland.



A comparison of simulations of pond evaporation (no emergent vegetation) with wetland (vegetation) evapotranspiration shows that ponds and wetlands have only minimal differences in water loss, around 2 mm per day on average (Figure 20). The result is rather surprising given Figure 19 above. However, the similarity can be explained by the relative ratios of vegetated and open water surfaces.

Figure 20

Evaporative water losses simulated for a pond (no vegetation) and a wetland (vegetation), Longford Park.



5.3.2 Wainoni Wetland 2

Like Longford Park, sensible heat is minor compared to latent heat over the water surface, the Bowen ratio is 0.26 on average. The emergent vegetation at Wainoni Wetland 2 is quite low and does not have the same level of exposure as the reeds at Longford Park. Hence the latent heat fluxes for open water and vegetation are fairly similar (Figure 21). However, the high degree of coverage by emergent vegetation means that vegetation has greater evaporative losses (Figure 22). The difference between simulated evaporative losses for the wetland and a pond (no emergent vegetation) is minimal.

Figure 21

Latent heat fluxes at Wainoni Wetland 2 .

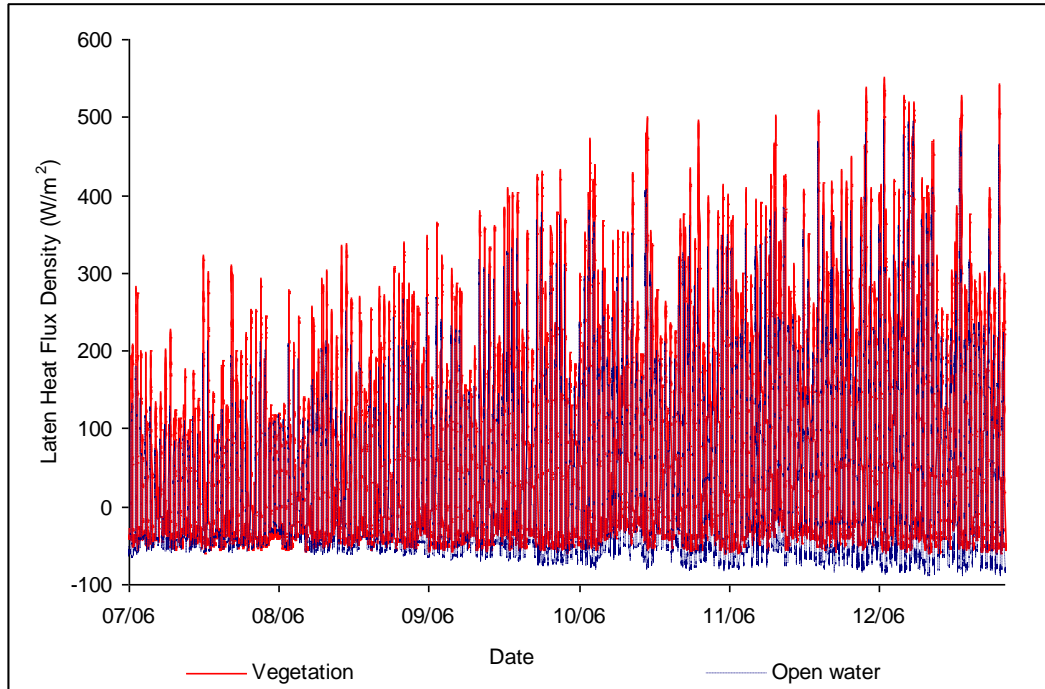
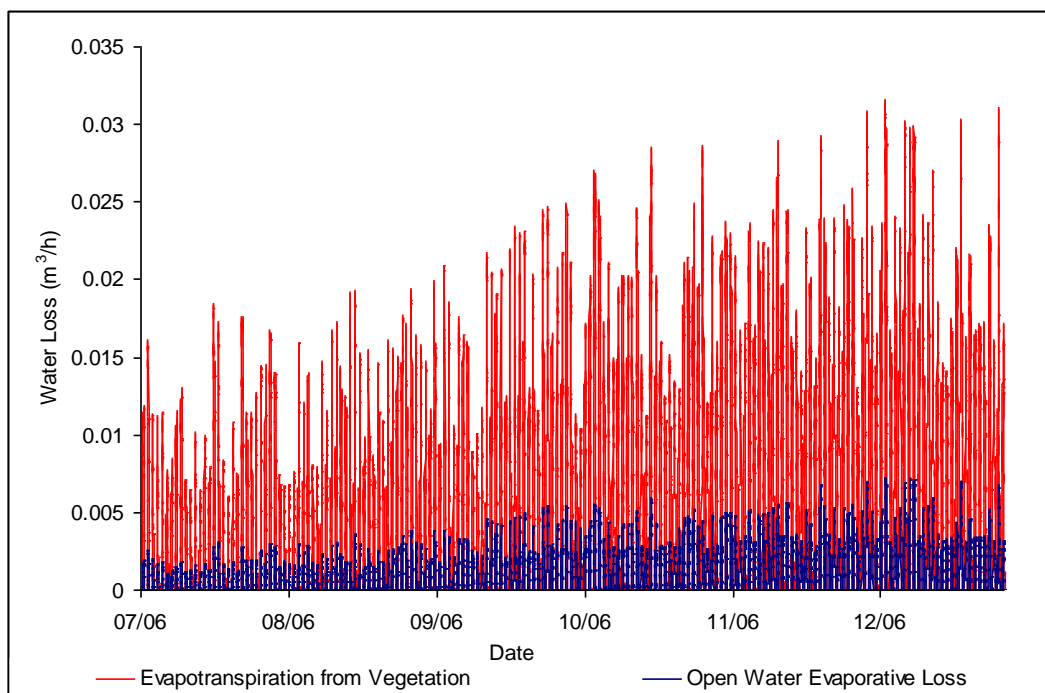


Figure 22

Evaporation and evapotranspiration from the different surfaces at Wainoni Wetland 2.



5.4 Flow reduction and attenuation

The model is run with discrete timesteps that may be greater than response time for larger events, especially when the wetlands are at full capacity. The flow sub-model stores water for each timestep which is released as a single point in time. That is, the weir and orifice equations are for instantaneous flow, and flow for each timestep is the instant flow value determined from the stored water multiplied by the length of the timestep. As a result, some of the simulated outflows peaks are greater than the inflow peaks. Part of the reason for choosing low run-off coefficients was to limit this effect as the lower coefficients smooth the peak flows without changing the flow volumes for each event. This artefact of modelling will vary depending on the outlet structure and the timestep.

5.4.1 Longford Park

The wetland flow simulation shows a rapid hydrological response to inflow with peak outflow coming in the next timestep (ie less than one-hour lag). The wetland generally attenuates the flow and, with the exception of a few of the larger events (see above explanation), flow peaks are reduced. Figure 23 shows simulated outflow against inflow for both the entire simulation period and for a series of flow events in early July 2004. Figure 23a. shows that some summer flow events seen at the inlet are either greatly reduced at the outlet or do not occur as a result of high evaporative losses in summer. The effect of evapotranspiration on flow is most noticeable from December through to April with no outflow simulated for some months. However, the high flows in autumn and winter are largely unaffected by evapotranspiration. If the model is run with evapotranspiration removed, the simulated outflow peaks are more or less unchanged during these seasons.

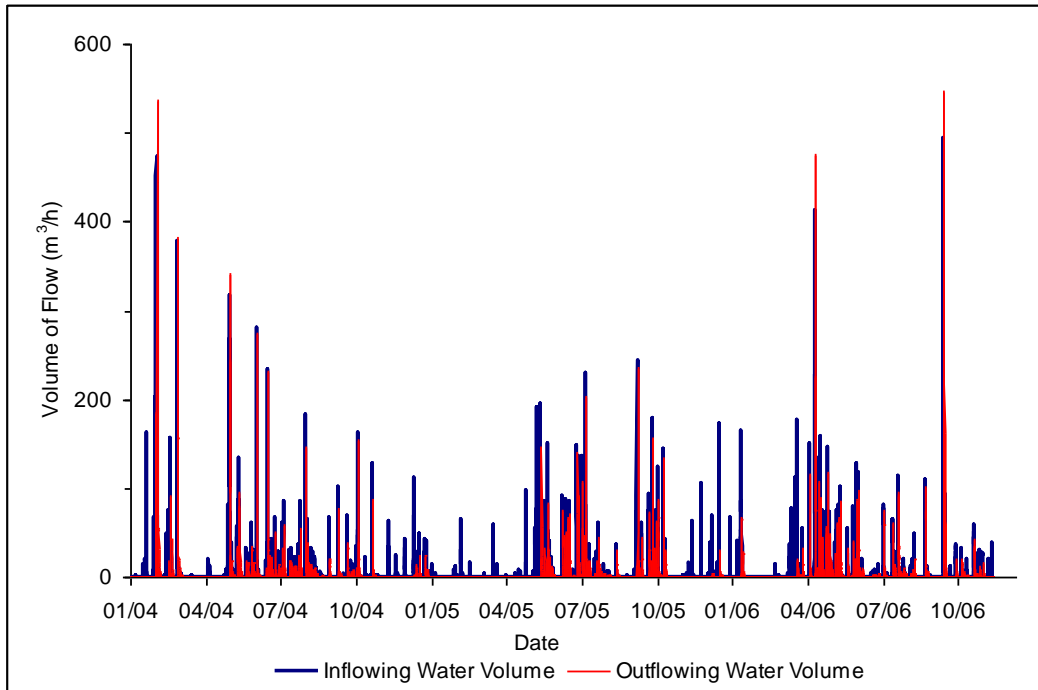
Figure 23b. shows the response timing and flow attenuation. Flow peaks at the outflow generally occur one or two timesteps after the inflow peak depending on the level of storage available at the beginning of an event.

Simulating the wetland as a pond has very little effect on flow. In terms of the water balance, the only difference between the two situations is the evaporative losses from water and emergent vegetation respectively. Figure 24 shows that a few summer outflow events are simulated for the pond but not for the wetland (December 30 2005, January 26 2005), other than that, the difference between flows is very minor.

Figure 23

Inflow and outflow simulated for Longford Park Wetland: a. 2004-2006; b. July 2004.

a.



b.

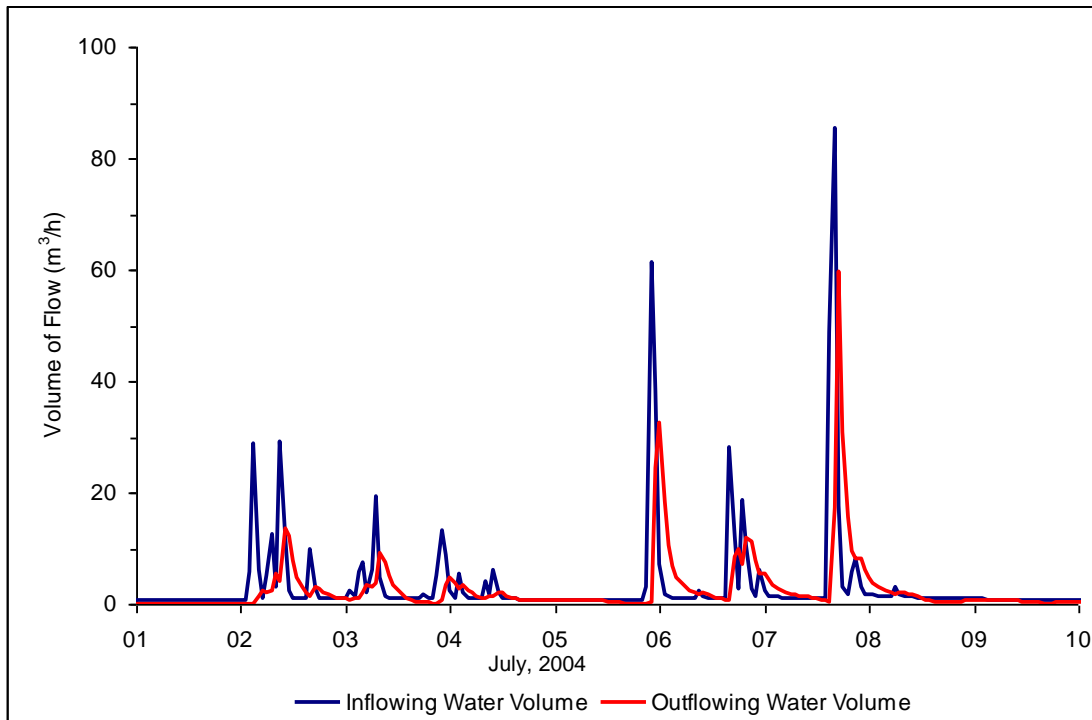
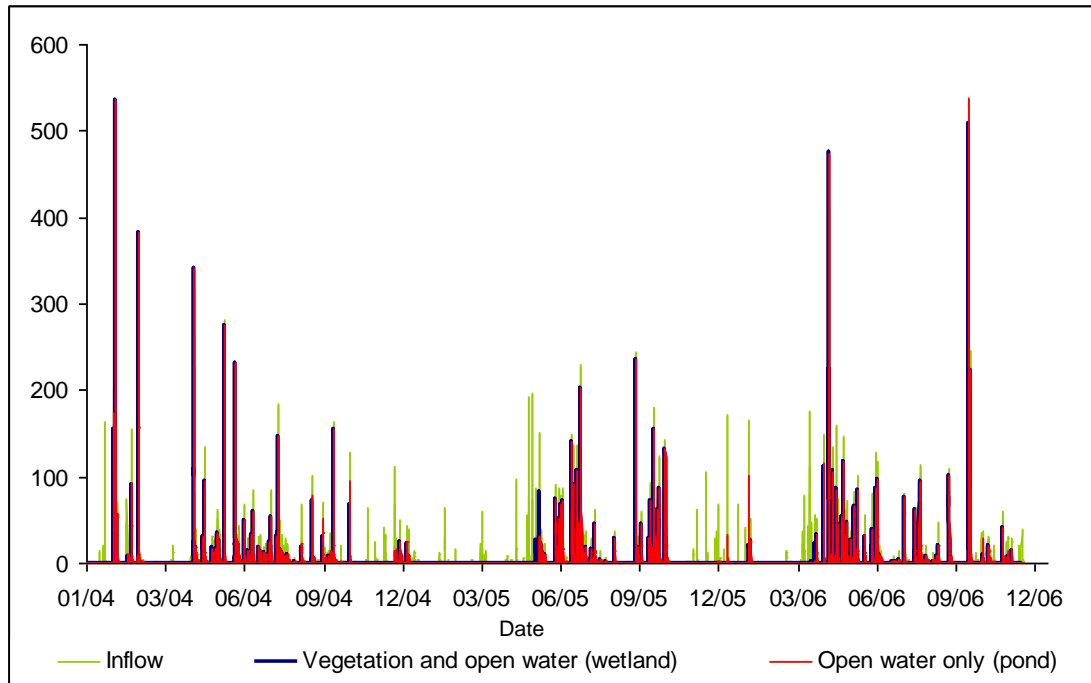


Figure 24

Inflow and outflow simulated for Longford Park Wetland with emergent vegetation (wetland) and without (pond).



5.4.2 Wainoni Wetland 2

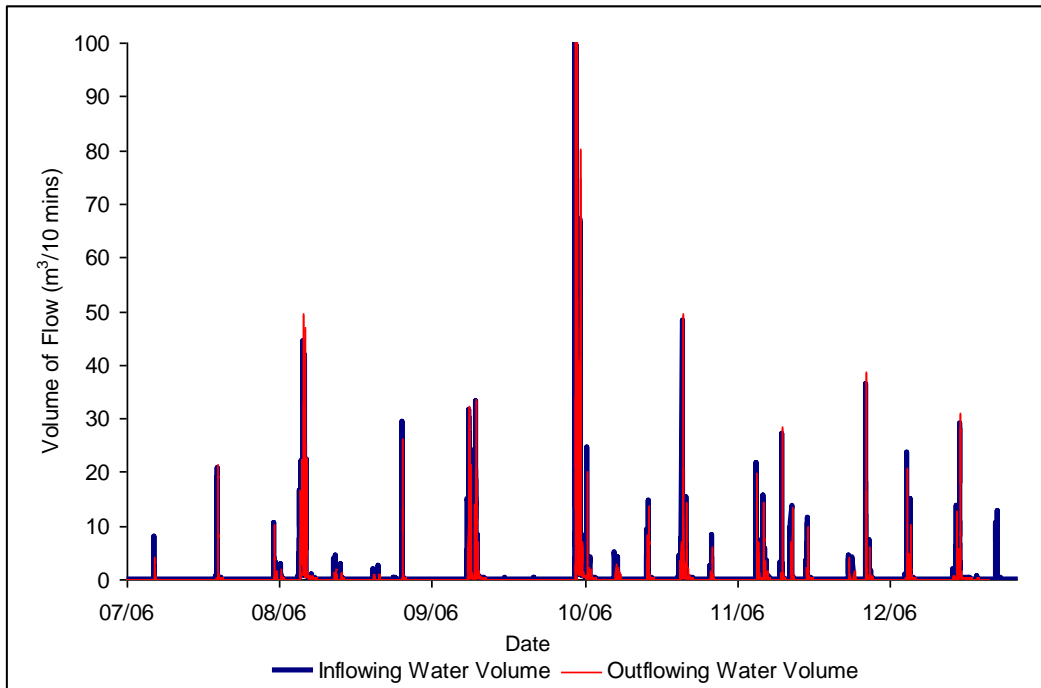
Wainoni Wetland 2 is small with limited storage yet the outflow structure is actually larger than the one at Longford Park. It is therefore not surprising that the simulated hydrological response seen in Figure 25 is almost instant. The total simulation period is displayed along with a flow event on 9 September 2006. It can be seen that during wet period, the wetland does not reduce flow peaks.

Figure 26 also suggests that the evaporative losses have only limited effect on outflow. The outflows for the larger inflow events are largely unaffected by evaporation. There are two summer inflow events in December 2006 that do not have simulated outflows. The no emergent vegetation (pond) simulation was very similar to the wetland simulation. Unlike Longford Park where the reeds are exposed to wind and radiation, the emergent vegetation is low and is also subject to shading and reduced sky-view. It should be noted that the simulation period does not cover January and February which are the warmest months. The differences between the simulated pond and wetland outflows in Figure 23 above for Longford Park occur during these high summer months. Moreover, both simulations suggest that some storm events can be mitigated by evaporative losses. Bearing in mind that Wainoni Wetland 2 is shallow, it is entirely plausible that the wetland could dry out attenuating flows generated by summer storms if the storms are spaced by sufficiently long intervals. Indeed, the last inflow event (December 28) is absent from the outflow simulations.

Figure 25

Inflow and outflow simulated for Wainoni Wetland 2: a. July – December 2006; b. August 5-8 2006.

a.



b.

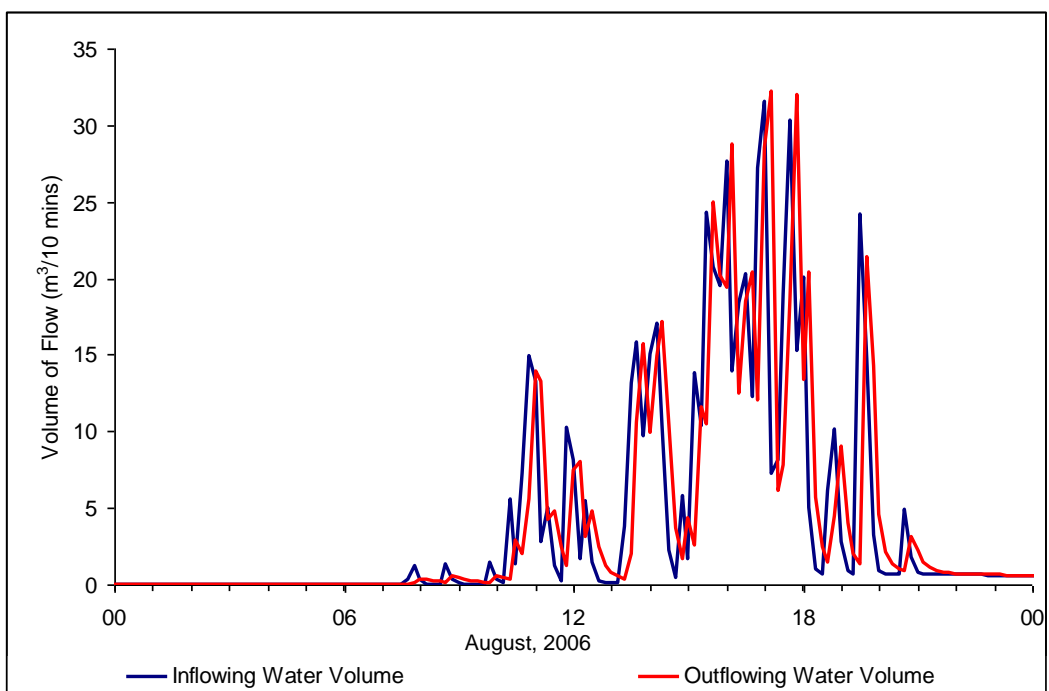
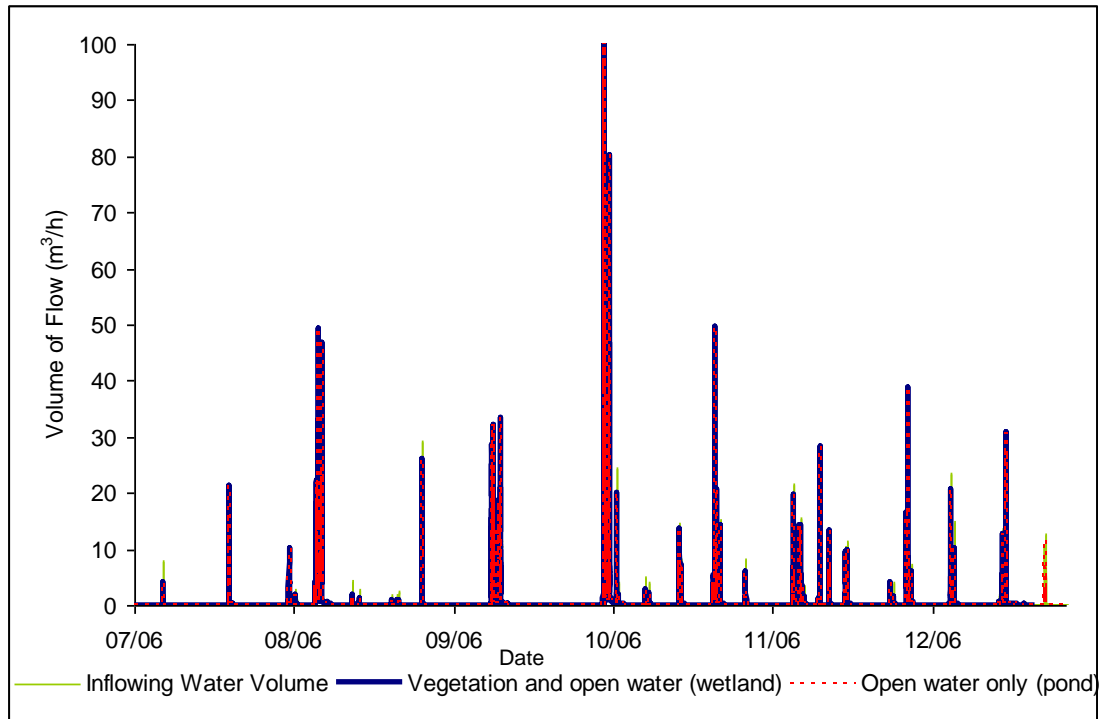


Figure 26

Inflow and outflow simulated for Wainoni Wetland 2 with emergent vegetation (wetland) and without (pond).



5.5 Implications for water management

5.5.1 Water temperature

Water temperature is an important part of the wetland energy balance as it affects longwave radiation emissions from the water surface and turbulent energy exchanges between the water and atmosphere. Water temperature is also important to wetland function: the warmer the water, the less dissolved oxygen it can hold but the greater the biological activity and the faster the settling rate.

The two wetlands have different exposure to solar radiation which has a great impact on water temperature. At Longford Park, the reduction of sky-view and shading are less than at Wainoni Wetland 2. The only sheltering of the water surface at Longford Park is from the emergent reed beds, which are quite low compared to the width of open water, whereas at Wainoni Wetland 2 is narrow and is ringed by vegetated banks which shelter both the water surface and emergent vegetation. As a result, Wainoni Wetland 2 exhibits a seasonal response to water temperature with respect to air temperature while there is no seasonality in the Longford Park. The Longford Park simulations suggest that water temperature is consistently several degrees warmer than the air temperature. Wainoni Wetland 2 has simulated water temperatures less

than air temperature in winter (low sun angles causing long shadows and low water albedo, longwave emissions greater than incoming longwave radiation leading to cooling) and greater in summer (high sun angles means solar radiation can rapidly heat the shallow water).

The model shows that water temperature is sensitive to water depth with Wainoni Wetland 2 (0.5 m depth) having a more rapid response to air temperature and greater diurnal ranges than Longford Park (1.5 m depth). This is in keeping with the findings of the US EPA (1999) for stormwater wetlands. Warmer temperatures can pose a problem downstream of the wetland by both increasing biological activity (eg, algal blooms) and reducing the amount of dissolved oxygen in water which can harm local biological communities and lead to fish death. Maxted *et al.* (2005) looked at the negative impacts of pond discharge (including stormwater ponds), which could be some 3 to 6 °C warmer than stream water on local macroinvertebrate species in the Auckland region. They found that while bank shading may reduce heating in smaller ponds, larger ponds were not sufficiently shaded to avoid heating. These findings are similar to the results above where Longford Park less response to shading and reduced sky-view than Wainoni Wetland 2.

5.5.2 Evaporation and evapotranspiration

The difference between evaporation from the open water surface and evapotranspiration from the emergent vegetation at Longford Park is more noticeable than at Wainoni Wetland 2 because the vegetation is not sheltered and has greater exposure than the water surface. At Wainoni Wetland 2, the emergent vegetation is low and is also sheltered by the bank vegetation. This means that the energy available for latent heat is very similar for both the water and vegetation. At both sites the latent heat over emergent vegetation is calculated with no stomatal resistance as the wetlands did not dry out. The resistance was taken from Acreman *et al.* (2003) who found that observed values had a wide spread seasonally and spatially for natural wetlands in the UK. Values between -50 and 100 were not unusual. If the resistance is set to just 25 s/m (the resistance for grass is around 70 s/m), there is no significant difference between water and vegetation. Setting resistance to 50 s/m decreases evapotranspiration compared to evaporation from the open water.

5.5.3 Flow

The wetlands have different responses at the outlet to inflow with the larger Longford Park wetland being better able to slow and attenuate flow than Wainoni Wetland 2. The latter has a large outlet structure (standpipe of 1.8 m diameter with debris screen, equivalent broad-crested weir length of around 4.8 m) compared to its dead storage (140 m³) and water entering the basin is able to flow through at the next timestep with very little reduction of the peak volumes. The former, on the other hand, is a larger wetland (2328 m³) with more regulated flow through a broad-crested weir (1.5 m).

The model was run for both wetlands with and without emergent vegetation to simulate wetlands and ponds. There is no doubt that wetlands and ponds have

different hydraulic behaviour, the emergent vegetation, meandering flow paths and submerged ridges associated on wetlands could improve removal efficiencies by encouraging plug flow and filtering suspended sediments. However, as outflow is a function of hydraulic head and the dimensions of the outlet structure, the simulations suggest that there is very little difference hydrologically. Full hydraulic modelling of the wetlands could give a different picture and may be an option for further study.

The simulations for both wetlands suggest that evapotranspiration from the emergent vegetation may be greater than evaporation from open water, though the results obtained are sensitive to the stomatal resistance in the model. The pond simulations (ie, no emergent vegetation) for both wetlands had similar outflows, that is, there was only a slight increase in flow peaks. During wet periods, the wetland has negligible evaporative losses between events and the water storage is kept at capacity. For both wetland and pond simulations for Longford Park, summer was marked by reduced flow with many summer events not causing flow to be simulated. The pond simulation had several minor summer events which were not present in the wetland simulation. The simulations at Wainoni Wetland 2 did not include mid to late summer. However, given that the wetland is shallow with very little storage, it can be speculated that the wetland could dry out between flow inflow events. There is an event in late December 2006 that was present in the pond simulation but not the wetland simulation. This suggests that there may be some differences in summer outflows for the two situations. It would be interesting to compare flows from Wainoni Wetlands 2 and 1 (similar dimensions and outlet structure but largely un vegetated) to see if the two facilities behave differently over summer.

The simulations for the wetlands (and ponds), suggest that evapotranspiration can reduce peak flows by lowering water levels between events. This is particularly noticeable at Longford Park where several years were simulated. Summer inflow events were often not present in the simulated outflow. While the reduction of flow peaks in summer due to evaporative losses may be good news in terms of erosion downstream, the reduction of flow could also be a problem as some urban streams, which would have had greater baseflow prior to urbanisation and may now experience summer low flows. This, coupled with heating in stream as well as the wetland could reduce water quality.

6 Conclusions

This project was commissioned by the ARC and accompanies a coupled energy and water balance spread-sheet model that has been applied to two wetlands. Wainoni Wetland 2 and Longford Park were chosen by the ARC as they represent the two types of wetland covered in TP 10 (trapezoid and banded bathymetry). Aside from bathymetry, the wetlands had different catchment areas and land use, dimensions, outflow structures, layouts and emergent vegetation – all of these effect both their energy and water balances. The main objective was to determine whether wetlands are more effective at controlling stormwater flows than ponds. Evaporation from open water and evapotranspiration from emergent wetland vegetation were thus prime considerations. Of concern to the ARC is the fact that stormwater can contribute to downstream channel and bed erosion – this means that design criteria for flow control should include adequate storage and flow regulation to avoid erosion in receiving streams.

This report describes the model including its organisation into sub-models, parameters and calculations. The model was used to simulate outflow from the wetlands with and without emergent vegetation. The latter was undertaken to allow a comparison with detention ponds of the same dimensions under the assumption that the two types of detention facility differ hydrologically only in evapotranspiration. As the model has not been calibrated, the findings listed below are tentative.

- The model is sensitive to the parameters which govern solar radiation absorption by the open water relative to the emergent vegetation (ie, shading and sky-view).
- With the default parameters, the emergent vegetation has a greater latent heat flux than open water, particularly at Longford Park where the reeds are about 1.2 m high above the water. At Wainoni Wetland 2, the emergent vegetation is low and the difference between the two surfaces is slight. However, this finding is tentative because the evapotranspiration sub-model is very sensitive to stomatal resistance. Changing this parameter within the range found in the literature has a great impact on the relative proportions of evaporation and evapotranspiration from the vegetation and water.
- For both wetlands, there is very little difference in the simulated evaporative losses for ponds and wetlands despite the difference in latent heat for open water and emergent vegetation. The lack of difference is due to several factors including the relative areas of open water to emergent vegetation, and changing patterns of shading for each type of detention facility.
- Simulated water temperature at Longford Park, where open water is more exposed to sun and wind, tracks the average daily air with a one or two day lag. The water temperature is around 2°C on average warmer than the daily average air temperature but can be up to 7°C warmer.
- Simulated water temperature at Wainoni Wetland 2 is sensitive to the height of the bank vegetation which shelters both the water surface and the emergent

vegetation. There is a seasonal difference in water temperature compared to air temperature. In winter when sun angles are low, the water temperature is less than air temperature. In summer the water is more exposed to solar radiation and warms above the air temperature.

- Water temperature is sensitive to the water depth, Wainoni Wetland 2 (depth 0.5 m) has a greater diurnal range of temperatures and responds more rapidly to changes in air temperature than Longford Park (1.5 m depth of open water pools).
- Outflow is governed by the storage available and the size and type of the outlet structure. The only water losses for a wetland system are deep percolation (usually minor) and evapotranspiration which is in turn dependant on energy availability and the relative covers of vegetation and open water..
- By increasing the amount of storage available during dry periods, evaporative losses do reduce flows from the wetlands. The Longford Park simulations found that peak flows during wet periods were largely unaffected while the pond had several summer flows not simulated for the wetland. Wainoni Wetland 2 was not simulated for high summer, even so, the flow event in late December 2006 was present in the pond simulations but not the wetland simulations.
- Longford Park, which is the larger of the two wetlands, is better able to attenuate peak flows. Wainoni Wetland 2 has a very large outlet structure despite its small size which means that the simulated outflow was almost instantaneous and inflows peaks were released in the next timestep.

7 Recommendations for Calibration and Testing

The focus of this project has been to simulate the hydrological differences between ponds and wetlands with an emphasis on evapotranspiration. The results and conclusion sections have stressed the need for model calibration and testing. Ideally, each of the sub-models should be calibrated separately. At the very least, flow and temperature observations are needed as these can be used as proxies for the full water and energy balances respectively. The different datasets should be from the same time period and should be of a sufficient length (at least six months to a year) to allow both calibration and testing during summer and winter. The normal method is to split the observation data sets into two, one half is then used to calibrate the model and the other to test. A common variant is to calibrate on a wet period and test on a dry period or vice-versa. The calibration and testing method chosen will depend largely on the length of the data record and the observations available.

Longford Park is in our view the more amenable to flow measurement both due to its size relative to Wainoni Wetland 2 and its inlet and outlet structures. It should also be noted, that of the two wetlands, Longford Park meets the criteria set in TP10 for a wetland despite its original design as detention pond.

7.1 Radiation

Simulated global radiation (ie, direct beam and diffuse solar) reaching Longford Park was compared to observations made at Auckland Airport and had good agreement. However, the degree of shading and sky-view have not been observed. Longwave radiation observations are also not available.

It would be feasible to measure both shortwave and longwave radiation at these wetland sites over periods of days to months using logging LiCor radiation sensors operated by NIWA, Hamilton. It is recommended that these data be complemented with synoptic surveys of shade using a hand held "canopy analyser" operated by NIWA, Hamilton. Estimates of shade could be made by measuring representative stem heights and stem densities and using a geometric shade model. This approach has been used for riparian tree shade with some success. Taken together, the three data sets would enable refined heat budgets to be developed, and the model thoroughly calibrated and tested.

Sky-view can be determined from photographs taken with a fish-eye lens at different distances from the banks and emergent vegetation.

7.2 Water temperature

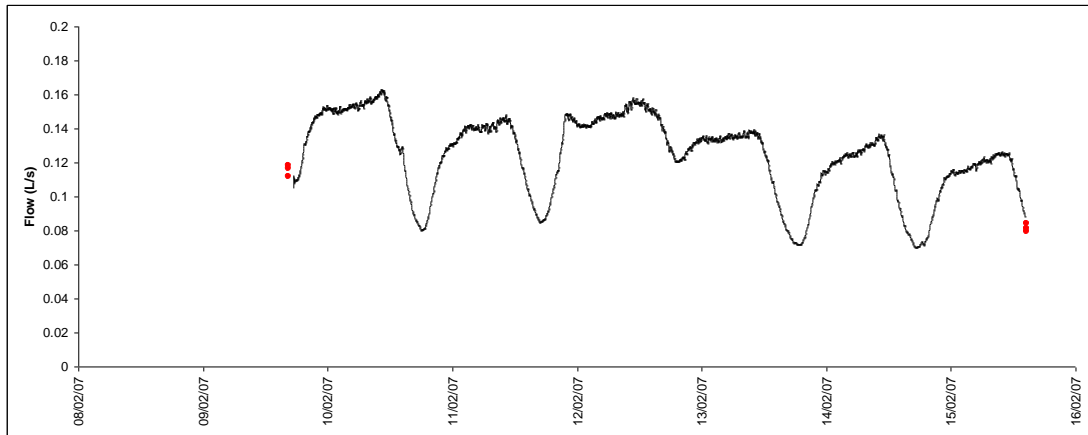
Absorption of solar radiation is largely responsible for raising water temperature and longwave emissions for cooling. Moreover, water temperature is one of the factors governing the transfer of the turbulent heat fluxes. This means that water temperature can be used as a proxy to give an indication of the wetland energy balance. Probes are available which can record continuous temperature and other water quality indicators (eg, conductivity, pH and dissolved oxygen) and could prove useful in determining the effectiveness of wetlands for improving water quality. These probes can be plugged directly into water samplers should sampling also be required.

7.3 Evapotranspiration

It is difficult to assess evaporative losses from a wetland directly from energy balance measurements. Open water can be reasonably equated to pan evaporation provided the wind fetch is long enough to reach equilibrium. However, wetlands are by definition covered with emergent vegetation which can be a barrier to wind and cause local turbulence. Moreover, this vegetation can have evapotranspiration rates different to the open water surface depending on the degree of exposure and the stomatal resistance to drying. Acreman *et al.* (2003) used eddy-correlation to determine the instantaneous turbulent fluxes over two natural wetlands in the UK. Evaporative losses can also be estimated as the residual of water balance studies where the difference between inflow and outflow volumes is taken into account are assigned to evapotranspiration. Where there is baseflow, the diurnal difference between inflows and outflows during summer low flows can give a very good indication of daily evapotranspiration. Rutherford (unpublished NIWA data) took flow measurements from a natural wetland near Taupo which clearly shows a diurnal fluctuation in discharge caused by evapotranspiration (Figure 27). However, as ponds and wetlands attenuate flow, losses over timesteps of less than a day cannot be determined with any real certainty. Moreover, as stormwater facilities are often designed without a baseflow component, the method may not be feasible for daily estimates and a longer timestep may be required. A very slight diurnal cycle in flow was simulated during lowflow periods by the model for Wainoni Wetland 2 which receives baseflow, but not for Longford Park where baseflow is minimal. Neither direct measurement of latent heat nor assessment from the water balance can be used to separate the relative contributions of open water or emergent vegetation where there is a mix of both covers. Despite the shortcomings, the residual method should suffice for daily estimates assuming that interactions with groundwater (baseflow from wetland margins and deep percolation) are negligible.

Figure 27

Discharge from Lost Lamb Wetland, Taupo, showing diurnal fluctuation caused by evapotranspiration, 9-15 February 2007.



7.4 Flow

Flow into and out of both wetlands should be monitored both to provide inflow data and for model calibration and testing. As noted above, flow data can also be used to determine long-term water losses due to evapotranspiration. If a stage recorder is used as part of flow measurement, this information can test whether the model is correctly simulating water storage which is a function of water level. For this project, the model has been run with inflow data which is itself modelled using the BECA run-off model which is subject to its own errors.

NIWA have the equipment and skills required for flow monitoring. Due to the configuration of the inflow and outlet structures, flow recording would be more reliable at Longford Park. Given the slow flow velocities at the wetland, a pressure transducer in the inflow pipe is not feasible. Instead, we propose a boxed weir like that constructed by NIWA for the ARC at the Henderson Vehicle Testing Station rain garden (Figure 28). A similar weir arrangement could be constructed in the outlet channel.

Figure 28

Boxed v-notch weir constructed by NIWA to monitor inflows at the Henderson Vehicle testing station (photo by Pete Pattinson).



8 References

- ACREMAN, M.C.; HARDING, R.J.; LLOYD, C.R. & MCNEIL, D.D., 2003. Evaporation characteristics of wetlands: experience from a wet grassland and a reedbed using eddy correlation measurements. *Hydrology and Earth System Sciences*, 7(1), 11–21 (2003).
- AKAN, A.O. & HOUGHTALEN, R.J., 2003. *Urban Hydrology, Hydraulics and Stormwater Quality*. John Wiley and Sons, INC. NJ, USA.
- ALLEN, R.G.; PEREIRA, L.S.; RAES, D. & SMITH, M., 1998. *Crop evapotranspiration - Guidelines for computing crop water requirements*. FAO Irrigation and drainage paper 56. Food and Agriculture Organization of the United Nations Rome.
- ANZECC, 1992. *Australian and New Zealand guidelines for fresh and marine water quality*. Australian and New Zealand Environment and Conservation Council & Agriculture and Resource Management Council of Australia and New Zealand, Canberra, Australia.
- AUCKLAND REGIONAL COUNCIL 1992. *Stormwater management devices: design guidelines manual. First Edition, TP 10*.
- AUCKLAND REGIONAL COUNCIL, 1999. *Guidelines for Stormwater Run-off Modelling in the Auckland Region, TP 108*.
- AUCKLAND REGIONAL COUNCIL, 2003. *Stormwater management devices: design guidelines manual. Second Edition, TP 10*.
- AUCKLAND REGIONAL COUNCIL, 2000. *Low Impact Design Manual for the Auckland Region, TP 124*.
- BAVOR, H.J.; DAVIES, C.M. & SAKADEVAN, K., 2001. Stormwater treatment: do constructed wetlands yield improved pollutant management performance over a detention pond systems? *Water Science and Technology*, 44:(11-12):565-570.
- BUTLER, D. & DAVIES, J.W., 2000. *Urban Drainage*. E & FN Spon, NY, USA.
- CAMPBELL, G.S., 1977. *An Introduction to Environmental Biophysics*. Springer-Verlag, New York.
- CHUNG, P. & FASSMAN, E., 2006. *Temperature effects of offline urban stormwater devices – project for ARC*.

- ELLIOTT, S.; HICKS, M.; DEBNATH, K.; WALTERS, R.; SHANKAR, U. & NIKORA, V., 2005. *Auckland urban stream erodibility investigations*. NIWA Client Report:HAM2005-031 (Prepared for ARC).
- EUGSTER, W.; ROUSE, W.R.; PIELKE, R.A.; MCFADDEN, J.P.; BALDOCCHI, D.D.; KITTEL, T.G.F.; CHAPIN, F.S.; LISTON, G.E.; VIDALE, P.L.; VAGANOV, E. & CHAMBERS, S., 2000. Land-atmosphere energy exchange in Arctic tundra and boreal forest: available data and feedbacks to climate. *Global Change Biology*, 6:84–115.
- FINCH, J.W. & GASH, J.H.C., 2002. *Application of a simple finite difference model for estimating evaporation from open water*. *J. Hydrol.* 255:253-259.
- HARRISON GRIERSON, 2001. *Kitto Block – Western Marsh – Maintenance Schedule*, Prepared for Universal Homes Ltd (provided by ARC).
- HARRISON GRIERSON, 2003. *Infrastructure Auckland Funding Application: Berlane Place and Longford Park Stormwater Quality Ponds*. Prepared for Papakura District Council (provided by ARC).
- HENDERSON-SELLERS, A. & ROBINSON, P., 1986. *Contemporary Climatology*. Longman Scientific and Technical, England.
- HENDERSON-SELLERS, B., 1984. *Engineering Limnology Pitman Advanced Publishing Program*, Boston.
- IDSO, S.B., 1981. A set of equations for full spectrum and 8-14 μm and 10.5-12.5 μm thermal radiation from cloudless skies. *Water Resources Res.* 17:295-304.
- JOWETT, I.G.; ELLIOTT, A., 2006. *Cohesive sediment design parameters for Auckland streams*. (NIWA client report HAM2006-108).
- LAFLEUR, P.M.; ROUSE, W.R. & CARLSON, D.W., 1992. Energy balance differences and hydrologic impacts across the northern treeline. *Int. J. Climatol*, 12, 193–203.
- MAXTED, J.R.; MCCREADY, C.H. & SCARSBROOK, M.R., 2005. Effects of small ponds on stream water quality and macroinvertebrate communities. *New Zealand Journal of Marine and Freshwater Research*, 39:1069–1084.
- MICHALSKY, J.J., 1988. The astronomical almanac's algorithm for approximate solar position. *Sol. Eng.*, 40:227-235.
- MITSCH, W.J. & GOSELINK, J.G., 1993. *Wetlands*. Van Nostrand Reinhold, New York. 2nd Edition.
- MONTEITH, J.L., 1965. Evaporation and the environment. *Proc. Symp. Soc. Experimental Biology*, 19:205-234.

- MONTEITH, J.L., 1981. Evaporation and surface temperature. *Q. J. Royal Meteorol. Soc* 107:1-27.
- MONTEITH, J.L., 1985. Evaporation from land surfaces: progress in analysis and prediction since 1948. *In Advances in Evaporation*, ASAE pp:4-12.
- OKE, T.R., 1987. *Boundary Layer Climates* (second edition). Methuen, New York.
- PENMAN, H.L., 1948. Natural evaporation from open water, bare soil and grass. *Proc. Royal Soc., London, Ser A*, 193:120-154.
- RUTHERFORD, J.C.; MARSH, N.A.; DAVIES, P.M. & BUNN, S. E., 2004. Effects of patchy shade on stream water temperature: how quickly do streams heat and cool? *Marine and Freshwater Research* 55:737-748.
- RUTHERFORD, J.C.; BLACKETT, S.; BLACKETT, C.; SAITO, L. & DAVIES-COLLEY, R.J., 1997. Predicting the effects of shade on water temperature in small streams. *New Zealand Journal of Marine & Freshwater Research* 31(5):707-721.
- SHUTTLEWORTH, W.J., 1993. Evaporation. In Maidment, D. (Ed), *Handbook of Hydrology*. McGraw Hill INC. USA.
- TIMPERLEY, M.H.; GOLDING, L.A. & WEBSTER, K.S., 2001. Fine particulate matter in urban streams: is it a hazard to aquatic life? *Second South Pacific Stormwater Conference Proceedings*, Auckland, New Zealand, 27 – 29 June 2001, pp:135-141.
- US NATIONAL HIGHWAY INSTITUTE, 2001. Urban Drainage Design Manual. *Hydraulic Engineering Circular No 22*, Second Edition.
- USEPA, 1999. *Storm water technology fact sheet: storm water wetlands*. EPA 832-F-99-025.
- WONG, M.H.; BREEN, P.F. & SOMES, N.L.G., 1999. Ponds vs wetlands – performance considerations in stormwater quality management. *Proceedings of the Comprehensive Stormwater and Aquatic Ecosystem Management, First South Pacific Conference*, Auckland, New Zealand, pp. 223-231.